RHEOLOGY AND PROCESSING OF NOVATEIN THERMOPLASTIC PROTEIN

THE UNIVERSITY OF
WAIKATO
Te Whare Wānanga o Waikato

A thesis

submitted in fulfilment

of the requirements for the degree

of

Master of Engineering

in Materials and Process Engineering

at

The University of Waikato

by

VELRAM BALAJI MOHAN

The University of Waikato,

Hamilton, New Zealand

September 2010

DEDICATED TO MY BELOVED PARENTS

(SH. S. MOHAN & SMT. R. MALINI)

ABSTRACT

Biopolymers have become suitable alternatives to petro-chemical polymers as they can biodegrade and are considered environmentally friendly. Novatein Thermoplastic Protein (NTP) is a newly developed plastic material using bovine bloodmeal. Knowledge of the rheology of NTP is required to assess processability and to optimise process design. The objective of this research was to use capillary rheometry and batch mixing to determine the rheology and processing behaviour of NTP. These were evaluated at constant plasticiser content, but using three different ratios of water to plasticiser (triethylene glycol, TEG). Each of these was evaluated at 115, 120 and 125 °C.

It was shown that NTP is a non-Newtonian, shear thinning fluid with similar behaviour compared to linear low density polyethylene. It was found that viscosity is highly dependent on water content; decreasing with increasing water content. At a shear rate of 15 s^{-1}, the apparent viscosity for the standard formulation (60 parts water per hundred parts bloodmeal) was 2000 Pa.s compared to 7000 Pa.s for the formulation containing 30 parts water [water (30) : TEG (30)], measured at 115 °C.

Viscosity decreased slightly with increasing temperature and the degree of non-Newtonian behaviour was mostly unaffected by temperature. The flow behaviour index, n, was found to be in the range 0.11 to 0.17, with no discernable temperature dependence. In the standard formulation, the total amount of plasticiser and ratio water to TEG was higher, which resulted in different flow behaviour with respect to temperature.

Batch mixing was used to determine the processing window (Δt) by monitoring torque changes over time during mixing. Processing window for standard NTP decreased from 260 to 220 seconds when the mixing speed was increased from 75 to 95 RPM.

The processing window was shortened with reducing water content or an increase in temperature. At 125 °C and 95 RPM the processing window was only 67 seconds for the formulation with 30 parts water and 30 parts TEG. It was concluded that crosslinking was accelerated with an increase in shear and temperature or a reduction in moisture content. Thermal or mechanical energy activates crosslinking, while water plasticises the polymer which decreases the rate of crosslinking.

Processing NTP required a delicate balance of supplying enough mechanical and thermal energy for chain rearrangement and consolidation, but preventing fast crosslinking. Crosslinking can be retarded using larger amounts of water, but excessive water may lead to problems after product moulding. Replacing water with TEG does not prevent crosslinking, but does lower the apparent viscosity during processing.

ACKNOWLEDGEMENTS

First and foremost, I would like to express my heartfelt thanks to my honourable academic supervisor, Dr. C. Johan Verbeek for his enthusiasm, endless help, encouragement and genuine advice throughout the period of the study. Without his help this research could not be possible and I totally inspired by his nature. I am also thankful to Mr. Paul Ewart for goodness of his heart and his support in this research.

My special thanks to science librarian, Ms. Cheryl Ward for her kind support in finding learning essentials. I am thankful to Mr. Alan Smith, Mr. Indar Singh, Mr. Steve Hardy, Mr. Stuart Finley, Mr. Brett Nichol and Mr. Chris Sistern for their technical support. I would like to thank Dr. Mark Lay for his timely help during the research.

I would like to thank Dr. P. Asokan, a visiting scientist to the Waikato University, for his help, moral support, care and wholehearted advice. I offer sincere gratitude to my friends N. Karpak, A. Sabar, S.S. Arun, R. Karthi, S. Refat, T. Tharik, A. Y. Suhail and S. Shahil for their hold up, help and encouragement. I am thankful to my plastic-research group members (especially Jim Bier) for their support and camaraderie.

I will be forever grateful to Mr. James Marris (HR- Pak ń Save, Clarence St.) for providing me part time employment which kept me fed during my study in New Zealand.

I would also like to thank, my brother-in-law Mr. A. Karthikeyan for helping my parents in my home country and my grandmother, Mdm. Muthamma Sethuraman for her personal support and encouragement. Finally I am really grateful to all the people who have helped me indirectly and whose name I cannot remember.

TABLE OF CONTENTS

LIST OF FIGURES

LIST OF TABLES

NOTATION

Ω	Angular speed
α	Aperture
°C	Degree Celsius
β	Density
γ_{true}	True shear rate
µm	Micro meter
Δ P	Pressure drop
Δ t	Processing window
γ	Shear rate
γ_w	Shear rate at wall
$\gamma_{apparent}$	Shear rate from experimental observation
τ	Shear stress
λ	Slope value
Γ	Torque
Γ	Maximum torque
η	Viscosity
τ_w	Wall shear stress
A	Area
BM	Bloodmeal
C_m	Moisture content
cm	Centimetre
DMA	Dynamic mechanical analysis
dt	Change of time
dy	Change of distance
dz	Change of displacement
F	Force
G	Gear ratio
g	Gram
H	Distance
Hz	Hertz

K	Flow consistency index
Kg	Kilo gram
L	Length
LLDPE	Linear low density polyethylene
m	Metre
M	Polymer melt consistency
Mc	Critical molecular mass
mm	Millimetre
M_m	Molecular mass
n	Flow behaviour index
N	Speed
NTP	Novatein thermoplastic protein
Pa	Pascal
pHr	Parts per hundred
Q	Volumetric flow rate
R	Radius
R_c	Radius of cone
R_e	External radius
R_i	Internal radius
RPM	Revolution per minute
s	Second
s^{-1}	Per second
SDS	Sodium dodecyl sulfate
SS	Sodium sulfite
t	Time
T	Temperature
TEG	Triethylene glycol
T_g	Glass transition temperature
t_{max}	Maximum time
t_r	Onset to consolidation
v	Volume
V	Velocity
V_s	Slip velocity

CHAPTER 1: INTRODUCTION

Polymers are very important for everyday life. Petroleum based polymers are most popular, widely used and commercially successful, owing to their excellent mechanical properties, durability, low cost and ease of processing. The major problem with many petroleum based polymers is their inability to degrade biologically, which harms the environment. In addition, there are limited petroleum resources available [1]. Due to these reasons biologically degradable and modified polymers from renewable resources (biopolymers) may be better alternatives. Among these, protein polymers have received greater attention during last couple of decades. Chemical and biological researchers are making rapid progress in the design and synthesis of protein plastics. Advances in polymer chemistry and bioengineering are converging towards the creation of useful bioinspired plastic materials with defined properties [2; 3]. Most of all, protein polymers are cost effective while meeting most of thermoplastic properties with degradability.

A challenge with protein polymers is to make them more processable since they have a complicated intermolecular structure. Processability of a material greatly depends on its rheology, i.e. flow behaviour [4]. Once the material's complete flow behaviour is determined, it is possible to control processability and set a standard operating procedure. For Newtonian fluids viscosity is independent of shear rate and time, whereas for non-Newtonian fluids viscosity it is dependent on shear rate and time. Proteins are typically non-Newtonian and shear thinning fluids.

Novatein Thermoplastic Protein (NTP) is a newly developed material by Novatein Bioplastic Technologies in Hamilton, New Zealand. The material is produced from bovine blood protein, which is a co-product of animal processing and most of its properties and applications and usages are unknown. Earlier studies focussed on optimising its formulation for mechanical properties and processing. It was demonstrated that the material could be extruded, injection moulded and compression moulded [5; 6; 7].

The main objective of this research was to understand and analyse the rheology of NTP. It will be assessed using capillary rheometry utilising combinations of water and plasticisers at different temperatures. Three formulations were considered in which the total amount of plasticiser was kept constant, but the ratio of plasticiser to water was varied.

Crosslinking time with respect to temperature and shear rate was assessed by monitoring torque changes during batch mixing to establish an appropriate processing window for NTP production. Viscosity data and results from batch mixer experiments can be used for further optimising process parameters during extrusion and injection moulding [8; 9].

CHAPTER 2: LITERATURE REVIEW

2.1 POLYMERS

Polymers are macromolecules formed by small monomers. There are two major types of polymers, synthetic (non-biodegradable) and natural polymers; a basic classification is shown in Figure 1.

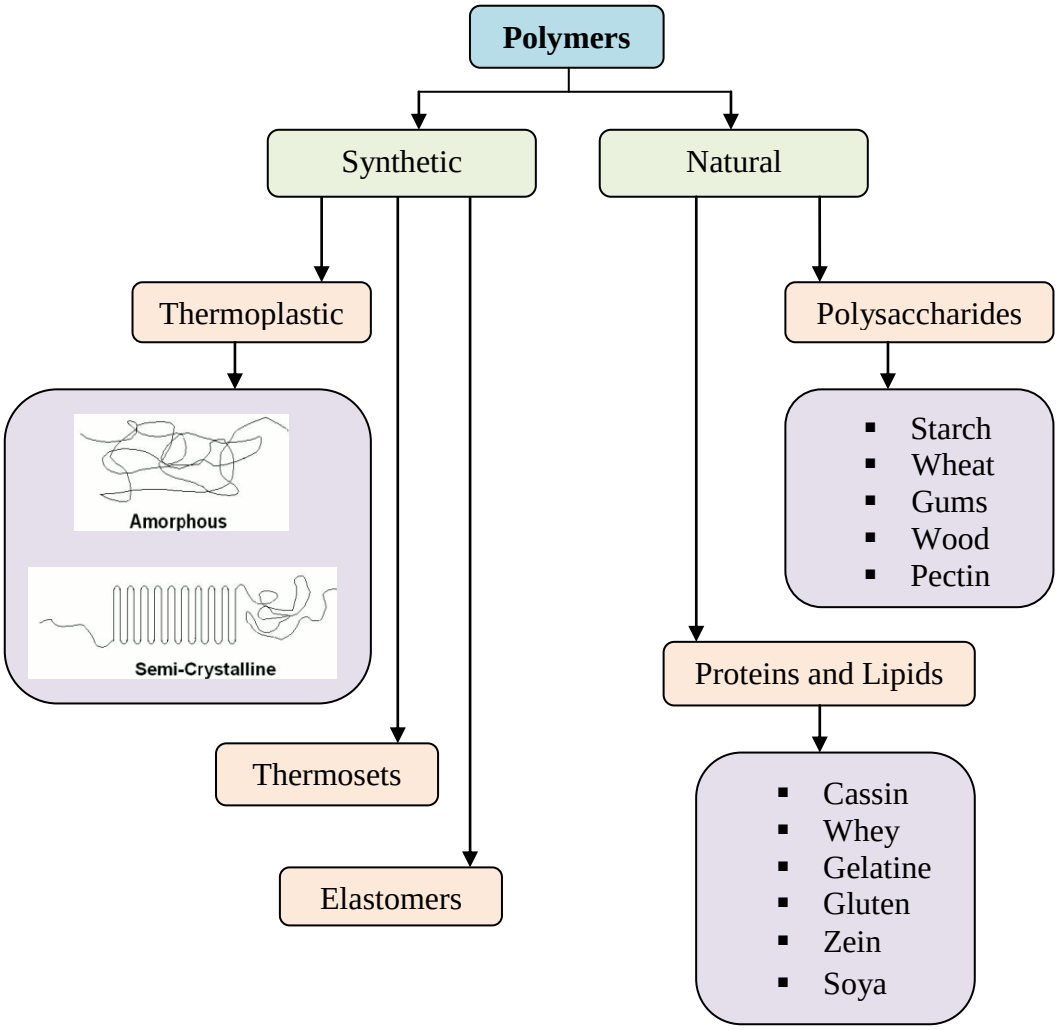

Figure 1: Classification of polymers [6; 10; 11]

Protein polymers, structure and property relationship

Protein polymers are natural polymers which can be obtained from plant and animal sources. Proteins can be a replacement for some petroleum-based polymers if they have the required physical and mechanical properties. Proteins are polymers consisting of 20 different amino acid monomers forming a polypeptide chain. It has four levels of structure; primary, secondary, tertiary and quaternary. A protein based material could be defined as a three-dimensional macromolecular network stabilised and strengthened by hydrogen bonds, hydrophobic interaction and covalent crosslinks [7].

Protein denaturation

Protein denaturation is important phenomena in protein processing which may lead to structural changes, thereby changes in processability.

During extrusion, proteins are denatured and transformed into a molten state. Denaturation is unique property of proteins and can be defined as the modification of secondary, tertiary or quaternary structures (Figure 2) of a protein molecule. The processability depends on the molecular mass and viscosity within the range of processing temperatures [5].

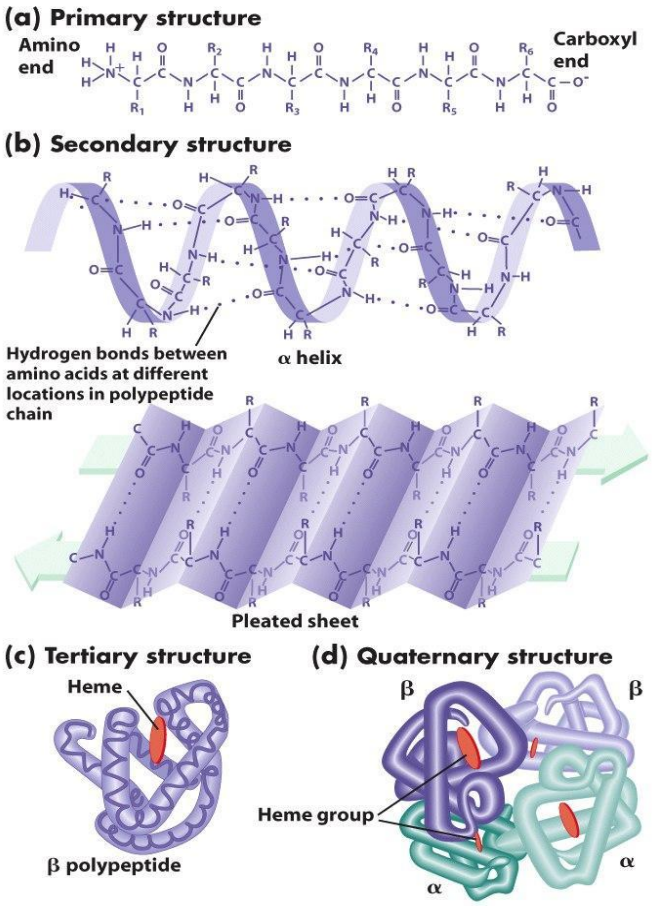

Figure 2: Protein structure [12]

The complex structure of the proteins makes it difficult to process them thermoplastically. The properties of a material greatly depend on it internal structure and molecular interactions. Since proteins have intricate chemical structures, improving its physical and mechanical properties are challenging. A basic key to improve the properties of protein polymers is to analyse and understand their processing characteristics, i.e. flowability and rheology. Rheology details are discussed in the following sections [10; 13].

Some protein sources that have been used to make thermoplastics are listed in Table 1.

Table 1: Some protein used as thermoplastics

Protein	Reference
Corn Gluten polymers	[10]
Collagen-based materials	[10]
Egg albumin	[10]
Peanut protein based polymers	[10]
Corn zein polymers	[14; 15]
Caseins	[16]
Fish protein	[17]
Keratin polymers	[18]
Soy protein polymers	[19; 20]
Whey protein polymers	[21]
Wheat Gluten polymers	[22; 23]
Blood protein polymers	[5; 24]
Feathermeal	[25]
Starch	[26]
Sunflower based protein	[27]
Oats protein	[28]

2.2 POLYMER PROCESSING

Extrusion, injection moulding and compression moulding are common methods to produce consumer products from plastics. Almost all thermoplastics have to be processed by extrusion at some stage of commercial manufacture. To improve the processing efficiency, understanding the flow behaviour of the material is very important. In principle, extrusion encompasses forcing a molten polymer through a shaped die by means of pressure at elevated temperature [29; 30]. Conventional processing methods are described below.

Extrusion

During extrusion, raw thermoplastic material in the form of small beads is gravity fed from a top mounted hopper into the barrel of the extruder. The material enters through the feed throat and comes into contact with the screw. The rotating screw forces the plastic beads forward into the barrel which is heated to the desired melt temperature. In most processes, a heating profile is set for the barrel in which independent controlled heater zones gradually increase the temperature of the barrel from the rear to the front. This allows the plastic beads to melt gradually as they are pushed through the barrel and lowers the risk of overheating which may cause degradation of the polymer. Extra heat is generated by the intense pressure and friction inside the barrel [29]. The typical extruder design is shown in Figure 3.

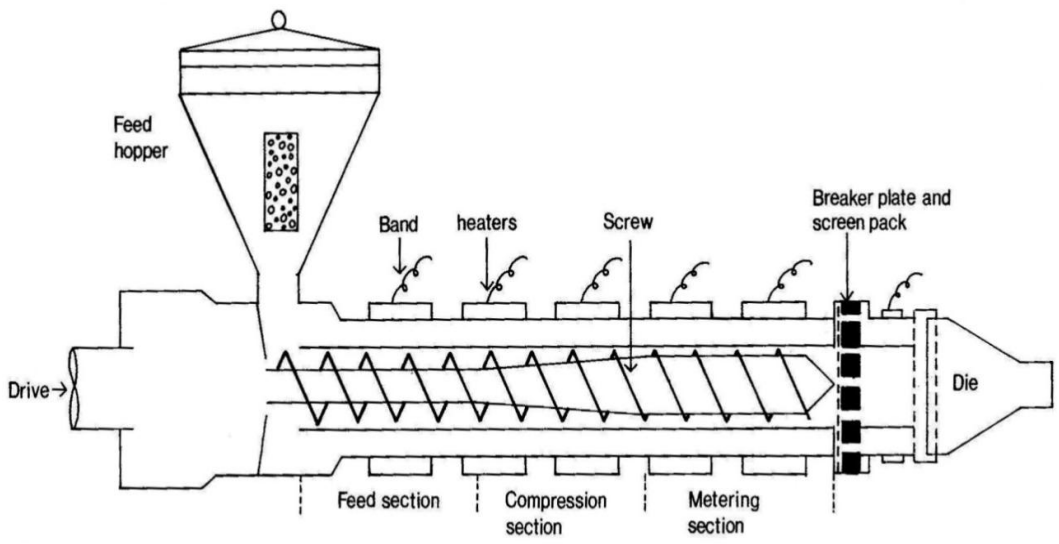

Figure 3: Extruder configuration [30]

Injection moulding

One of the common methods of shaping polymer is injection moulding. An injection moulding machine comprises four zones: feed zone, heating zone, injection zone and moulding zone, which are referred in Figure 4.

The mould has two halves, a fixed half and a moving half. The moving half is attached to the moving platen where as the fixed half is attached to the stationary platen (Figure 5A). A typical laboratory injection moulding machine is shown in Figure 5B.

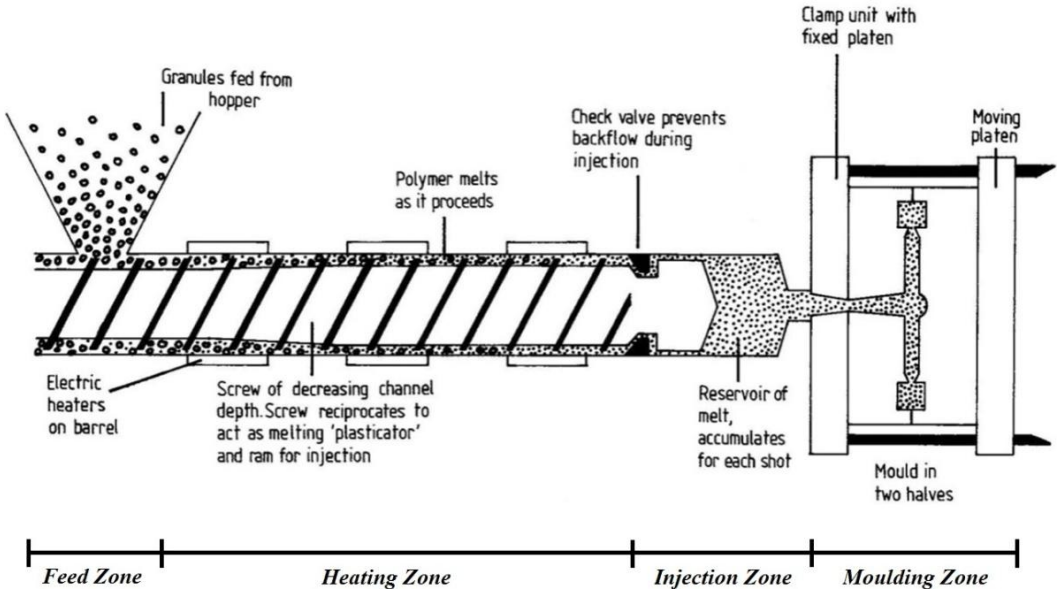

Figure 4: Injection moulding units [30]

Material is fed to the machine through a hopper. Colorants are usually fed to the machine directly after the hopper. Polymer enters the injection barrel by gravity through the feed throat. Upon entrance into the barrel, the polymer is heated to the appropriate melting temperature. The polymer is injected into the mould by a reciprocating screw or a ram injector. The reciprocating screw offers the advantage of being able to inject a smaller percentage of the total shot. Finally the material is ejected after cooling [31; 32; 33].

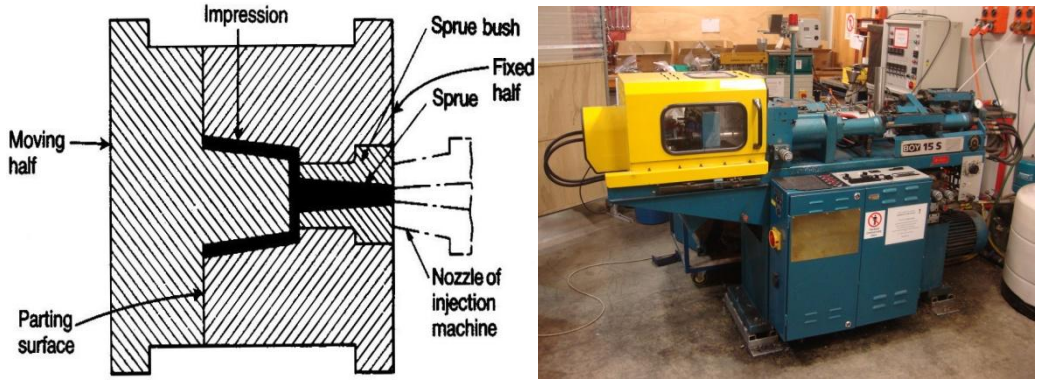

(A) **(B)**

Figure 5: A) Injection mould halves [33] B) a laboratory injection moulding machine

Compression moulding

Compression moulding is another widely used manufacturing method. Compression moulding equipment consists of a matched mould, a heat source, and some method of exerting force on the mould halves. The polymeric material is placed between the mould halves, compressed under heat and then cooled. The compression pressure can be varied as required. Typically, compression is produced by a hydraulic ram. For severe moulding conditions, moulds are usually made of various grades of tool steel [30; 31; 34]. The typical design of the machine and technique are shown in Figure 6.

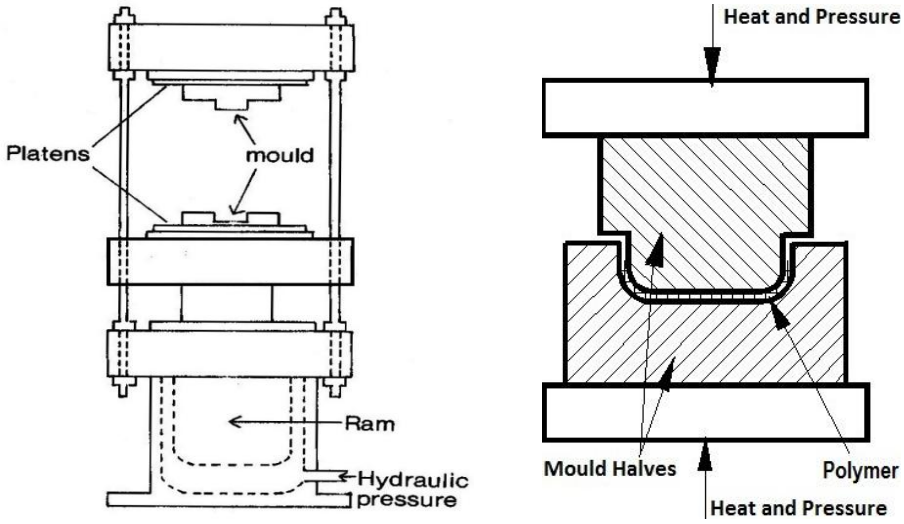

Figure 6: Compression moulding machine and technique [30; 35]

Viscosity and polymer processing

Polymer viscosity has great implications in polymer processing. Melt viscosity is important for efficient machine, mould and die designs [36]. Typical shear rates differ for each processing method and conditions. A few typical processes are shown in Table 2. High rates of shear are not necessarily involved in high processing speeds (high volume throughput). The viscosity of a polymer system is reliant on the processing method and is not constant; the apparent viscosity depends on shear rate and will be further discussed in Section 2.3.

Table 2: Viscosity ranges for different processes [30]

Process	Shear rate (s^{-1})
Compression moulding	1 - 10
Calendaring	10 - 100
Extrusion	100 - 1000
Injection moulding	$1000 – 10^5$
Reverse roll coating	3×10^3

2.3 RHEOLOY FUNDAMENTALS

Rheology is the study of flow and deformation of a material and how that flow is affected by stress, strain and time. The term ‘rheo’ means ‘to flow’ [37].

2.3.1 Viscosity

A basic definition of viscosity is a material’s resistance to flow. This is indicative of magnitude of forces needed for flow. Flowability or flow behaviour of fluids is characterised by the viscosity that describes the internal resistance of the melt to an externally acting load.

High viscosity of materials requires more energy for processing and flow through narrow spaces or tight corners may be difficult. It is important to know how viscosity changes with temperature and processing rate for efficient process and mould design [38].

Consider, a Newtonian fluid, placed between two parallel plates with separation distance (H), in which the top plate is moving to the right with constant velocity (V). Under steady state conditions, the fluid is subjected to a shear force (F), (Figure 7).

A friction force will develop at the contact surface in the direction opposite to motion and movement will be resisted by the viscous reaction in the fluid. This viscous reaction is proportional to the material's shear viscosity [38].

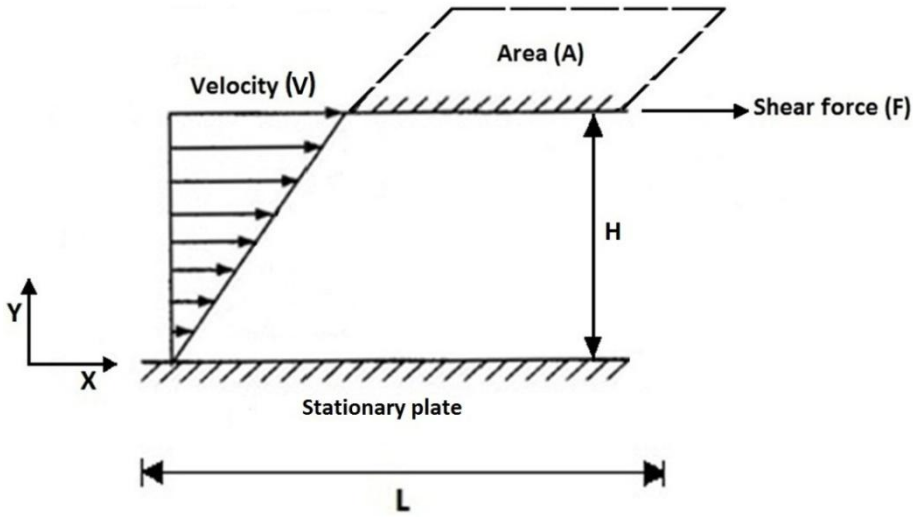

Figure 7: Principle of viscosity [8]

Shear stress can be found from the force, F, acting on the moving plate and its area, A.

$$\text{Shear stress } (\tau) = \frac{F}{A} \text{ Nm}^{-2} \quad (1)$$

The shear rate is found from the velocity 'V' relative to distance 'H' (Equation 2).

$$\text{Shear rate}(\gamma) = \frac{V}{H}\ (s^{-1}) \quad (2)$$

Shear rate may be expressed as the velocity gradient in the direction perpendicular to the shear force.

$$\tau \propto \left(-\frac{dV}{dH}\right) \quad (3)$$

Equation (3) states that the shear force per unit area is proportional to the negative of the local velocity gradient. This is known as 'Newton's law of viscosity' [39]. In the Equation 4, η is the proportionality constant between shear stress and shear rate. This proportionality constant is called the viscosity of the fluid.

$$\tau = \eta\gamma \quad (4)$$

Typical viscosities for a range of substances are listed in Table 3.

Table 3: Viscosity ranges for different polymer systems [30]

Substance or system	Viscosity (MPa)	Consistency
Air	10^{-5}	Gaseous
Water	10^{-3}	Fluid liquid
Polymer latex systems	10^{-3} - 10^{-1}	Liquid
Olive oil	10^{-1}	Liquid
Paints	10^{-2} - 10^{-1}	Creamy
PVX plastisols	1-3 x 10^{-1}	Paint-like
Glycerol	10	Thick
Resins for resin/glass	50	Syrup
Golden syrup	10^{3}	Syrup
Liquid polyurethanes	10^{2} – 10^{3}	Syrup
Polymer melts	10^{2} – 10^{6}	Toffee
Rubber before cure	10^{2} – 10^{6}	Stiff plasticine
SMC, DMC (moulding compounds)	10^{2}	Dough
Pitch	10^{9}	Flowing solid
Glass	10^{21}	Rigid solid

Tensile viscosity

Sometimes polymer materials are deformed not in shear, but in tension, such as in blow moulding of plastic bottles. For these situations, the tensile viscosity is defined as [30]:

$$\text{Tensile viscosity } (\eta) = \frac{\text{Tensile stress}(\tau)}{\text{Tensile strain rate } (\gamma)} \quad (5)$$

2.3.2 Newtonian and non-Newtonian behaviour

It was shown in the previous section that for a flowing fluid the shear stress is proportional to the shear rate. When this relationship is linear, the fluid is called a Newtonian fluid and the viscosity was defined by Equation (4). For a non-Newtonian fluid, shear stress versus shear rate is non-linear where the apparent viscosity is not constant at a given temperature and pressure but it is dependent on flow geometry, shear rate and time.

Apparent viscosity is the ratio of shear stress (τ) and shear rate (γ) as given by Equation (6):

$$\text{Apparent viscosity } (\eta) = \frac{\text{Shear stress}(\tau)}{\text{Shear rate } (\gamma)}$$

$$\eta = \frac{\tau}{\gamma} \text{ (Pa. s)} \quad (6)$$

The flow behaviour of most thermoplastics does not follow Newton's law of viscosity. These materials are conventionally grouped into three types:

- Fluids whose properties are not reliant on time under shear are called 'time-independent fluids'.

- Fluids whose properties are time dependent under constant shear are called ‘time-dependent fluids’.

- Fluids exhibiting characteristics of both ideal fluid and elastic solids and showing partial elastic recovery, after deformation are categorised as ‘visco-elastic fluids’ [36; 39].

2.3.3 Time-independent behaviour

For time-independent fluids, viscosity is not a function of time, but dependent on the shear rate. Most complex substances, like polymers, are likely non-Newtonian, for which viscosity is not constant and the flow behaviour must be characterised by measurements of apparent viscosity at different shear rates.

These fluids are further divided into three classes:

- Shear thinning or pseudoplastic
- Shear thickening or dilatant
- Visco-plastic

Shear thinning or pseudoplastic

The most common type of time-independent non-Newtonian fluid behaviour observed is pseudo-plasticity or shear–thinning, characterised by an apparent viscosity which decreases with increasing shear rate (Figure 8).

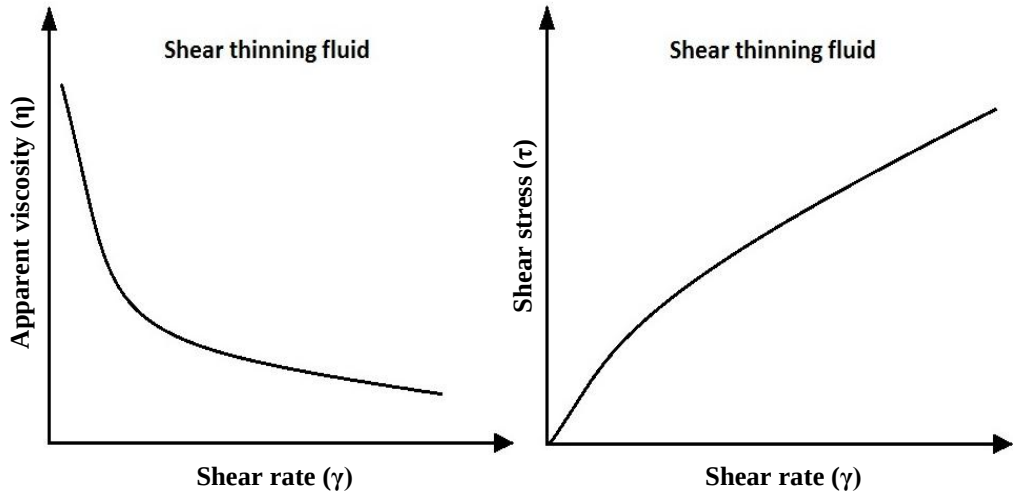

Figure 8: Viscosity vs. shear rate and shear stress vs. shear rate (Shear thinning)

Both at very low and at very high shear rates, most shear-thinning polymer solutions and melts exhibit Newtonian behaviour, as shown in Figure 9 [38].

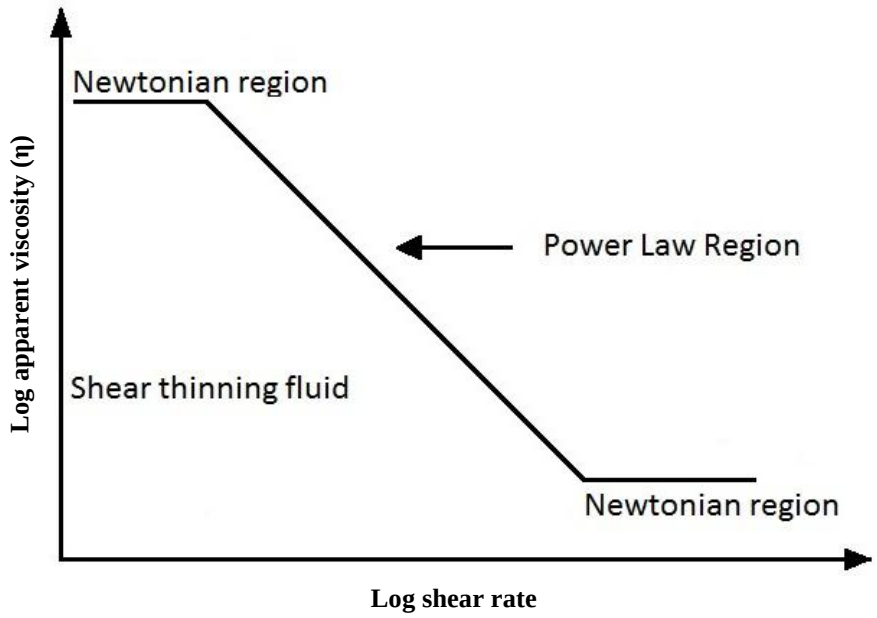

Figure 9: Viscosity regions for a shear thinning fluid [40]

Shear thickening or dilatant fluids

Dilatant fluids are similar to pseudoplastic systems, but their apparent viscosity increases with increasing shear rate. This type of fluid behaviour was originally observed in concentrated suspensions [30; 36]. A typical shear rate vs. shear stress diagram is shown in Figure 10.

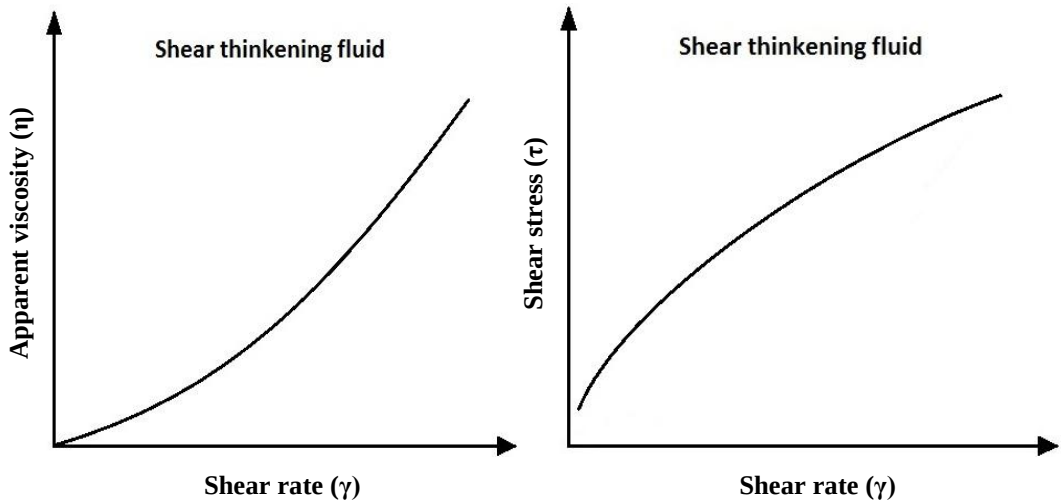

Figure 10: Viscosity vs. shear rate and shear stress vs. shear rate (Shear thickening)

Visco-plastic

This type of fluids behaviour is characterised by the existence of a yield stress (τ_0) which must be exceeded before the fluid will deform of flow [11]. This kind of material will deform elastically when the externally applied stress is smaller than the yield stress. These materials also called Bingham plastics and its flow curve is shown in Figure 11.

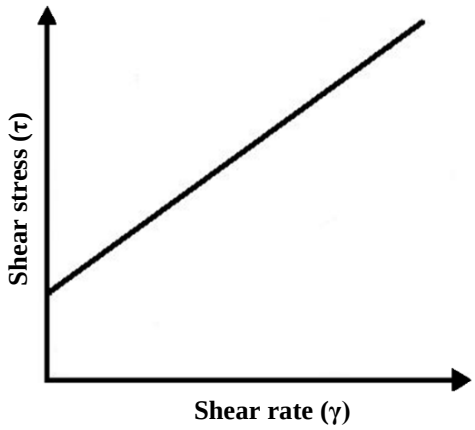

Figure 11 Bingham or viscoplastic behaviour [37]

2.3.4 Time- dependent behaviour

In practice, apparent viscosities may not only depend on the rate of shear, but also on the time the fluid has been subjected to shear [36]. These are further classified as thixotropic and rheopectic fluids.

Thixotropic fluids

A material is said to exhibit thixotropy if, when it is sheared at a constant rate, its apparent viscosity (or equivalent shear stress) decreases with time.

Rheopectic fluids

The relatively few fluids for which the apparent viscosity increases with time of shearing are said to display rheopexy or negative thixotropy. Figure 12 shows typical representation of time-dependent fluid behaviour [41].

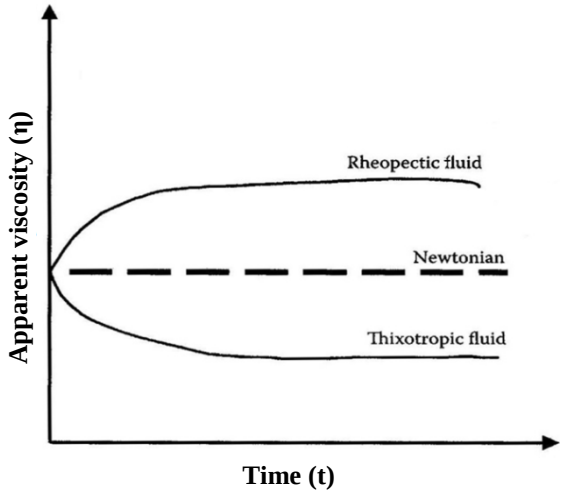

Figure 12: Viscosity vs. time at constant shear rate for rheopectic and thixotropic fluids [41]

2.3.5 Visco-elastic fluids

Substances exhibiting characteristics of both ideal fluids and elastic solids and showing partial elastic recovery, after deformation, are categorised as visco-elastic fluids [36].

2.4 RHEOLOGY MEASUREMENT

The relationship between shear stress and shear rate for describing the flow behaviour of a polymer melt can be measured by the following rheometry setups [37; 38]:

- Rotational rheometers
- Capillary rheometers
- Falling-sphere viscometers and
- Extensional rheometers

2.4.1 Rotational rheometry

Rotational rheometers generally have two rotational-symmetric components mounted on a common axis, with the fluid to be characterised between them. The measuring principle of the rotational rheometers is standardised in ISO 3219. For determining flow characteristics, there are two ways to make use of the geometry on which the rotational rheometers are based:

- CS-rheometers (CS=Controlled Stress): Shear stress is specified and the velocity gradient is determined proportional to viscosity.
- CR-rheometers (CR=Controlled Rate): Shear rate is specified and the resulting shear stress is determined [38].

Rotational rheometers are classified based on the geometry of the setup.

- Cone-plate rheometers
- Plate-plate rheometers
- Coaxial cylinder rheometers

Cone-plate rheometers

Cone-plate rheometers consist of a horizontal base plate on which the polymer is placed and allowed to reach the required test temperature. The cone, having a vertical axis, is lowered into the centre of the polymer melt until its tip just contacts the metal plate. The cone is then made to rotate either at fixed torque or fixed speed of rotation. The angle, α, that the cone makes with the plate is usually less than 5°, to ensure uniform and simple shear (shown in Figure 13).

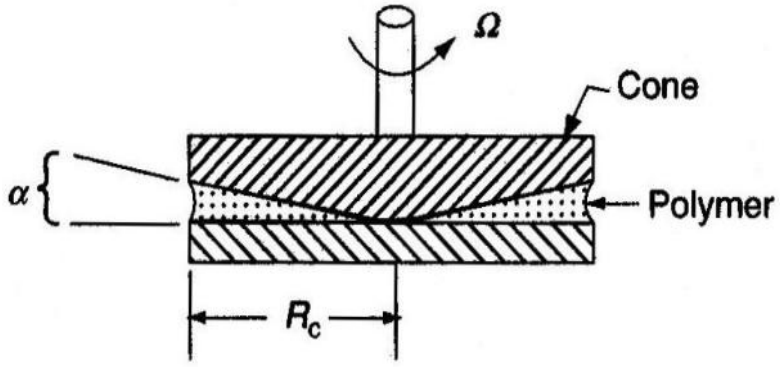

Figure 13: Cone plate rheometry [36]

If the rate of rotation of the cone is dθ/d*t*, and torque (Γ), angular speed (Ω), aperture (α) and radius of the cone (R_c) are known then shear stress (τ) and shear rate (γ) is given by Equations 7, 8 and 9 [37; 38],

$$\text{Shear stress } (\tau) = \frac{\left(\frac{d\theta}{dt}\right)}{\alpha} = \frac{\Omega}{\alpha} \ (s^{-1}) \quad (7)$$

$$\text{Shear rate } (\gamma) = \frac{3\Gamma}{2\pi R^3} \ (\text{Pa}) \quad (8)$$

$$\text{Viscosity } (\eta) = \frac{(3\Gamma\alpha)}{2\pi R^3 \Omega} \ (\text{Pa.s}) \quad (9)$$

Coaxial cylinder rheometers

These rheometers involve two coaxial cylinders, the outer one being fixed (vessel like), and the inner one being rotated at constant rotational speed, or at constant torque. The cylindrical vessel has a radius R_a and the internal cylinder has radius R_i. Torque and rotational speed can be related to shear stress and shear rate (Method-DIN 53 018). Shear stress can be generated by rotating either the external (Couette type) or the internal (Searle type) cylinder. Schematic representation of a coaxial rheometry is shown in Figure 14.

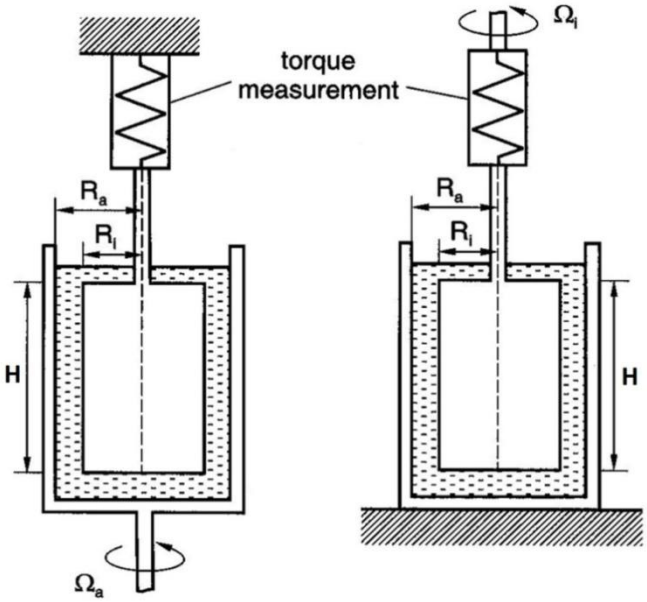

Figure 14: Coaxial (Couette & Searle) type rheometers [38]

The basic mathematical equations for this rheometry are as follows [38]. The known parameters, angular velocity of internal cylinder ($\Omega_i = 0$), angular velocity of external cylinder (Ω_a), radius of both internal and external cylinders and height of the cylinder (H) are combined with measured torque (symbols are defined in Figure 13):

$$\text{Shear stress } (\tau) = \frac{\Gamma}{2\pi R^2 H} \text{ (Pa)} \qquad (10)$$

$$\text{Shear rate } (\gamma) = \frac{2\left(\mathrm{Ra}^2 - \mathrm{Ri}^2\right)}{\left(\mathrm{Ra}^2 - \mathrm{Ri}^2\right)}\Omega \ \ (\mathrm{s}^{-1}) \tag{11}$$

$$\text{Viscosity } (\eta) \ = \frac{\Gamma\left(\mathrm{Ra}^2 - \mathrm{Ri}^2\right)}{4\pi r^2 \mathrm{H}\ \mathrm{Ra}^2 \mathrm{Ri}^2 \Omega} \ \ (\mathrm{Pa.s}) \tag{12}$$

Plate-plate rheometers

These rheometers are characterised by two plane parallel plates with radius R at a distance H between them. In this arrangement, the velocity gradient depends on the radius of the rotating upper plate and the height of the gap. The shear rate in a plate-plate arrangement can be varied by changing the distance between plates or the angular velocity over a very large area. In contrast to cone-plate type rheometry, the shear rate in plate-plate rheometers varies with varying radii [37]. In Figure 15, the equipment is illustrated and parameters are indicated, where Γ is torque, R is the radius of plates, H is the distance between the two plates and Ω is the angular velocity.

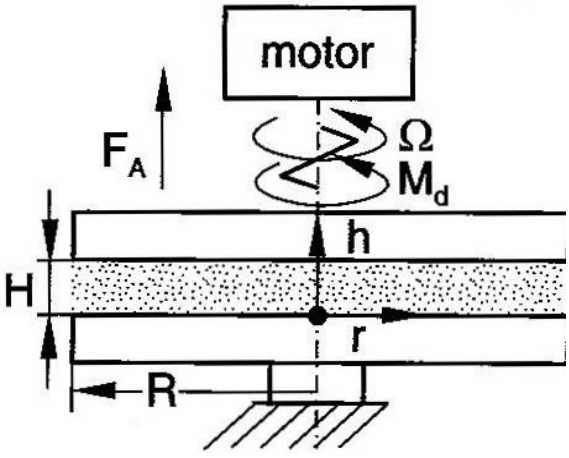

Figure 15: Plate-plate rheometry [38]

The equations for the determination of flow properties are:

$$\text{Shear stress } (\tau) = \frac{2\Gamma}{\pi \mathrm{R}^3} \ (\mathrm{Pa}) \tag{13}$$

$$\text{Shear rate } (\gamma) = \frac{R\Omega}{H} \ (s^{-1}) \quad (14)$$

$$\text{Viscosity } (\eta) = \frac{2r}{\pi R^4 \Omega} \ (\text{Pa.s}) \quad (15)$$

2.4.2 Capillary rheometry

Capillary rheometry is an effective engineering tool for real time viscosity measurement and control for polymer melts during processing. Many rheological measurements have been made with capillary rheometry as its accuracy is better compared to cone-plate and strain controlled rheometric techniques. Moreover, capillary rheometry can predict sensitive changes in viscosity through temperature and strain changes.

Capillary rheometers can be divided into the following types:

1. Low pressure capillary rheometers.

- Ostwald type
- Ubbelohde type
- Cannon-Fenske type

2. High pressure capillary rheometers

- Intermittent (Cylinder-Piston system) with variable piston force
- Intermittent (Cylinder-Piston system) with variable piston speed
- Continuous (Cylinder-Screw system) [38].

This study focussed a high pressure capillary type which is most relevant to polymer melts.

Screw driven capillary rheometry

Capillary rheometry is characterised by the fact that the fluid to be investigated flows through a capillary having circular cross section, a heating barrel (cylinder) to heat the polymer and a piston or plunger to push the polymer melt through the capillary. Capillary rheometers can be used with low or high viscosity polymer melts, solutions or dispersions [42; 43].

A screw driven capillary rheometry can either be a single or twin screw extruder. The reservoir or barrel is connected to heating elements for temperature control. At the die, a removable capillary is fixed. A pressure sensor is mounted at the entrance of the die, in order to calculate the pressure drop across the capillary [19]. Volumetric flow rate (Q) can easily be varied by varying the RPM. A typical laboratory capillary rheometry is shown in Figure 16.

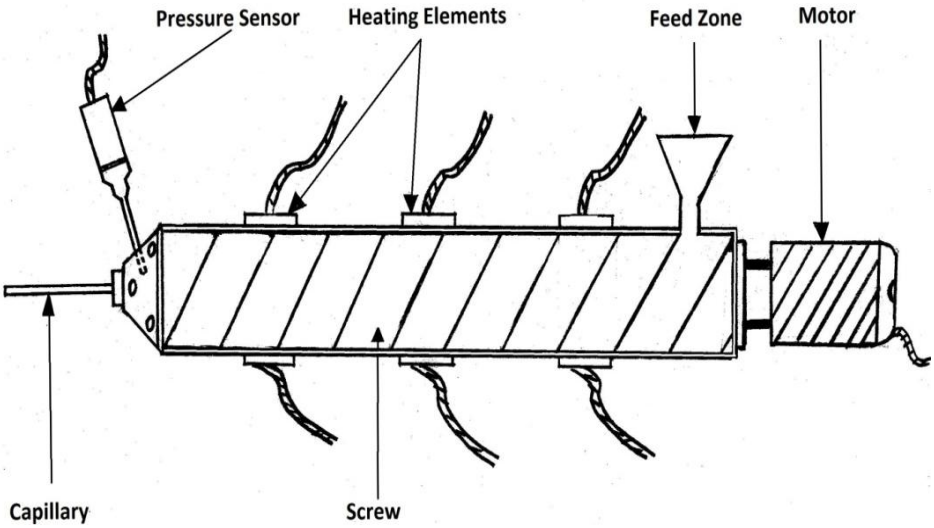

Figure 16: Capillary rheometer

When pressure (P) is applied to the polymer melt at the entrance of the capillary, there will be an energy loss (owing to friction) while the melt travels through the capillary length (L) (Figure 17). The frictional energy loss is directly proportional

to the viscosity of the fluid. By the time the end of the capillary has been reached, the pressure corresponds to atmospheric pressure. Viscosity can be determined if pressure drop, length, radius of the capillary and volumetric flow rate are known [38].

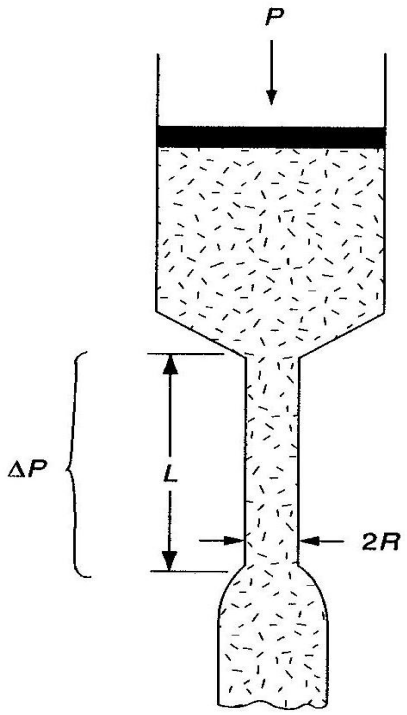

Figure 17: Mechanism of capillary rheometry [37]

Advantages of capillary rheometry [22; 44; 45]

- Low cost
- Accurate prediction of viscosity
- Simple configuration
- Easy to relate results to the properties of the studied material
- Suitable for operation at high temperature
- Suitable for polymer melts

Shear rate, shear stress and apparent viscosity

The main objective in rheometry is to measure the relationship between the applied force and flow rate for a given polymer melt at the required temperature. These measurements provide data for design of standard operating procedures during processing and may also describe a fundamental property of the polymer which may relate to its macromolecular structure [46].

Assuming, no end effects at the capillary die, shear rate and shear stress for fully developed Newtonian flow could be calculated as [38; 47]:

$$\text{Shear stress } (\tau) = \frac{\text{Force}}{\text{Area}}$$

$$= \frac{(\Delta P\, \pi\, R^2)}{2\pi\, R\, L}$$

$$\tau = \frac{\Delta P\, R}{2L}\ (\text{Pa}) \qquad (16)$$

Where;

R→ Radius of the capillary (mm)

L→ Length of the capillary (mm)

ΔP → Pressure drop (Pa)

(ΔP) = (Pressure at exit – Pressure at entrance)

Hence, $\Delta P = P_2 - P_1$ (Pressure at exit corresponds to atmospheric pressure)

If the velocity distribution is fully developed and parabolic (Figure 18), the shear rate can be calculated by Equation 17 [48],

$$\text{Shear Rate } (\gamma) = \frac{4Q}{\pi R^3}\ (s^{-1}) \qquad (17)$$

Where;

Q→ Volumetric flow rate (mm^3/sec)

R→ Radius of the capillary (mm)

In Figure 18, the region of flow in which the effects of the viscous shear forces caused by fluid viscosity are manifested is called the "velocity boundary layer or boundary layer". These layers also cause the fluid particles in the adjacent layers to slow down gradually as a result of friction. The initial region at the entrance is called "irrotational flow" [42].

The region from the pipe inlet to the point at which the boundary layer merges at the centreline is called the "hydrodynamic entrance region". The region beyond the entrance region in which the velocity profile is fully developed and remains unchanged is called the hydrodynamically fully developed region [36].

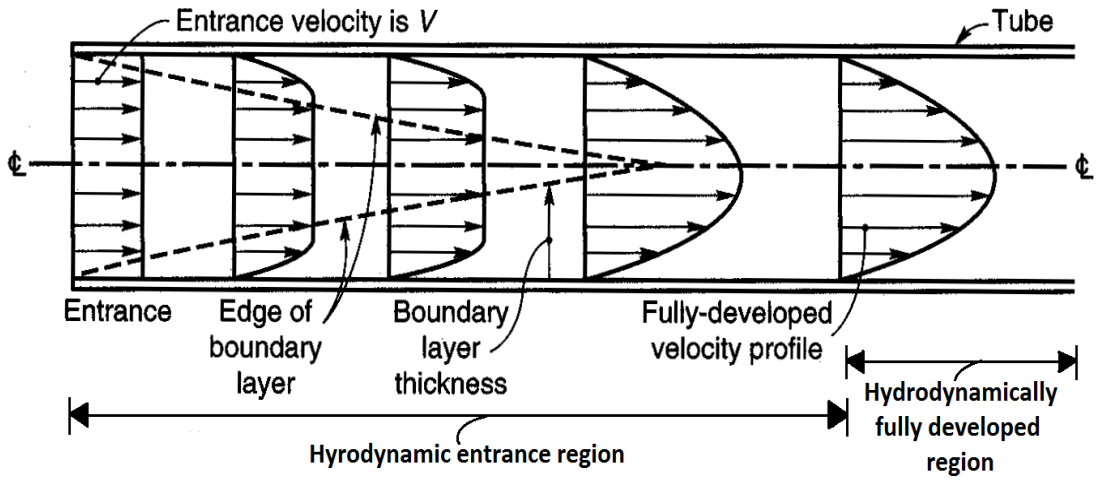

Figure 18: Development of the boundary layer and velocity profile for laminar flow in the entrance region of a pipe [36; 42]

Knowing the shear rate and shear stress, the apparent viscosity (η) for non-Newtonian fluids can be calculated using Equation (18).

$$\text{Apparent viscosity } (\eta) = \frac{\text{Shear Stress}(\tau)}{\text{Shear rate } (\gamma)} \tag{18}$$

$$\eta = \frac{\tau}{\gamma} \text{ Pa. s}$$

$$= \frac{(\Delta P \, R / 2L)}{(4Q / \pi R^3)}$$

$$\eta = \frac{\pi \, R^4 (\Delta P)}{(8QL)} \text{ Pa. s}$$

The above equation forms the basis of capillary rheometry, which is known as the Hagen Poiseuille's equation for determining viscosity of a fluid when channel dimensions are known [36; 38; 39].

The apparent shear viscosity (η) of a non-Newtonian fluid can also be described as a function of the shear rate in terms of a power law model:

$$\eta_a = K \, \gamma_a^{n-1} \tag{19}$$

or shear stress as a function of shear rate:

$$\tau_a = K \, \gamma_a^{n} \tag{20}$$

Usually the Power law model is expressing in logarithmic form as [51]:

$$\text{Log } \eta_a = n \text{ Log } \gamma_a + \text{Log } K \tag{21}$$

Where;

K→ Flow consistency index.

n→ Flow behaviour index (n=1 for Newtonian and n<1 for non-Newtonian)

Exit and entrance effects

Exit and entrance effects are consequences of the fact that near the entry to the capillary tube, the flow is not fully developed and the pressure drop is increased. The magnitude is dependent on the type of non-Newtonian fluid [36]. According to Bagley [49], there will be some energy loss when a polymer melt is forced from large extruder or barrel diameter to a relatively small diameter of the capillary. This makes it difficult to measure true shear rate and true viscosity. The pressure drop occurs at the entrance to the capillary section mainly because the cross section of a capillary is generally much smaller than that of a reservoir [50; 51], which is illustrated in Figure 19. These effects also depend on length of the capillary. However, the contribution to the exit effect is usually negligible as long as the length-to-radius ratio (L/R) of the capillary of the order 100-120.

There are three types of corrections used in capillary rheometry:

- Bagley correction corrects entrance and exit effects by compensating energy losses
- Rabinowitsch correction corrects shear rate at the wall
- Mooney analysis corrects shear rate as a result of wall slip

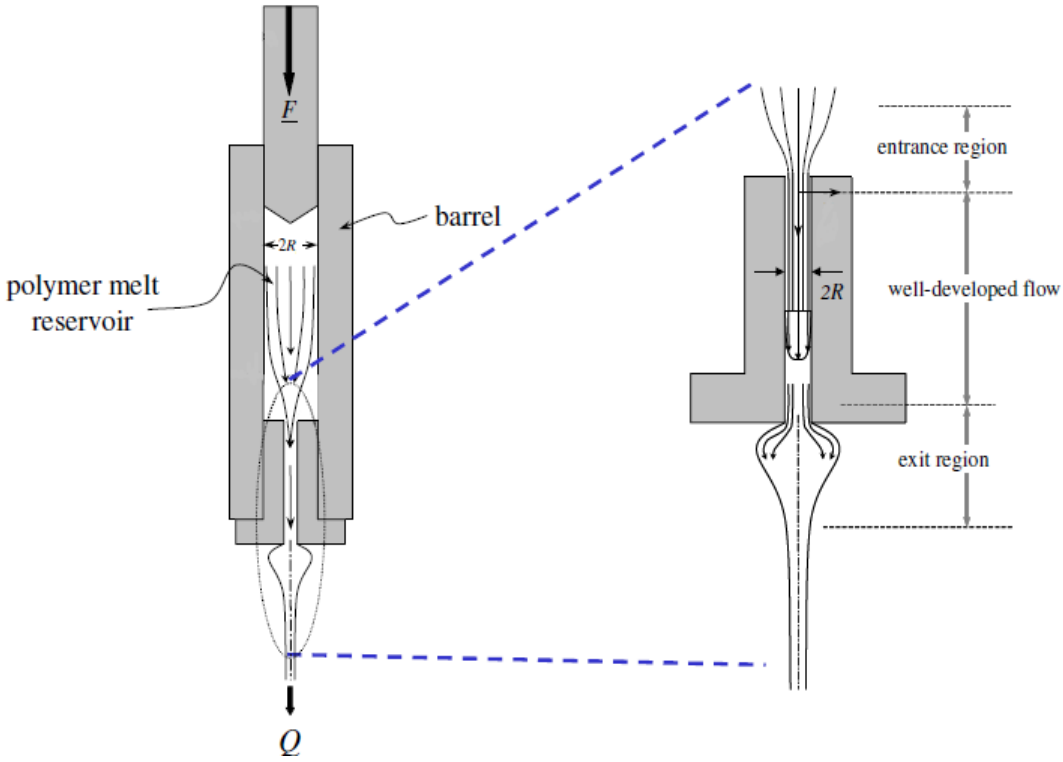

Figure 19: Flow effects in capillary [52]

Energy losses can be corrected by the following procedures proposed by Bagley and Rabinowitsch [19; 49]. For non-Newtonian fluids those corrections can be applied if they obey the power law model for apparent viscosity [19; 47; 53].

The Bagley correction predicts an effective shear stress by assuming an effective capillary length, $(L+\lambda R)$, greater than the actual capillary length. The greater or extra length corresponds to the overall energy loss at the entrance of the capillary when calculating pressure drop (ΔP) (Figure 20). Hence, measurements using more than two capillary lengths should be made.

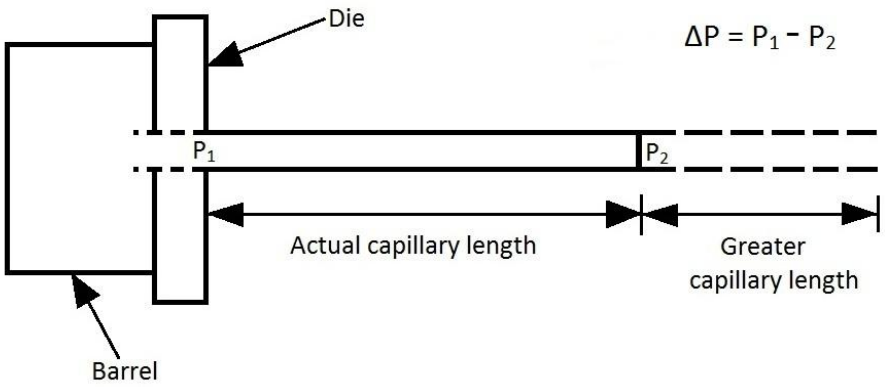

Figure 20: Pressure drop for capillary rheometry

The true shear stress can then be calculated from the Equation 22 as,

$$\tau_{true} = \frac{\Delta P}{2\left[\left(\frac{L}{R}\right)+\lambda\right]} \text{ (Pa)} \quad (22)$$

At a constant shear rate the pressure drop (ΔP) required to produce this shear rate should be a linear function of length to radius (L/R). By extrapolating to ΔP = 0, the value of 'λ' can be obtained from the slope at the particular shear rate [49; 54; 55].

Rabinowitsch has proposed a correction to account for the error between the apparent shear rate, i.e. shear rate obtained from experimental observation and the true shear rate. The power law model is used to determine the flow behaviour index 'n', which is then used to correct the experimental shear rate values using Equation 23. The equation is called the Rabinowitsch correction [19].

$$\gamma_{true} = \left[\frac{3n+1}{4n}\right] \gamma_{apparent} \ (s^{-1}) \quad (23)$$

Where;

γ_{true} = True shear rate

$\gamma_{apparent}$ = Shear rate from experimental observation

n = Flow behaviour index, calculated from power law model (Equation 21)

In capillary rheometry, homogeneous shear is difficult to achieve due to wall slip. Wall slip occurs due to flow instabilities that lead to distortions at wall surface and it reduces shear rate at the wall. Prior studies linked these instabilities to slip of the polymer melt relative to the solid surfaces of the extruder. This leads to velocity profile rearrangement, thereby errors in interpreting experimental measurements may occur.

In capillary rheology, wall slip is likely to give rise to a situation when the data for wall shear stress (τ_w) and wall shear rate (γ_w = V/R) obtained with capillaries of different diameters appear to be inconsistent even after the results have been corrected for all other known effects. Wall shear rate is a function of wall shear stress and it is given by:

$$\left(\frac{V}{R^3}\right)\frac{1}{\tau_w} = \frac{(V_S)}{R\tau_w} + \frac{Q}{\tau_w\,\pi R^3}\ (s^{-1}) \tag{24}$$

Where;

Q→ Volumetric flow rate

τ_w→ Wall shear stress

V→ Actual velocity

V_s→ Slip velocity

R→ Radius of the capillary

It is customary to quantify the effect of wall slip by assuming a slip velocity, V_s at the wall (Figure 21). Slip velocity can be obtained from the slope of (V/R) versus (1/R) for different capillary diameters. This implies that at the wall of the channel

fluid velocity $V_z = V_s$. Finally, wall shear rate can be calculated from Equation (26). This analysis is called Mooney analysis [52; 56; 57; 58; 59; 60].

$$\gamma_{wall} = \frac{(V - V_s)}{R} \ (s^{-1}) \tag{25}$$

Where;

V→ Velocity without slip

V_s→ Velocity with slip

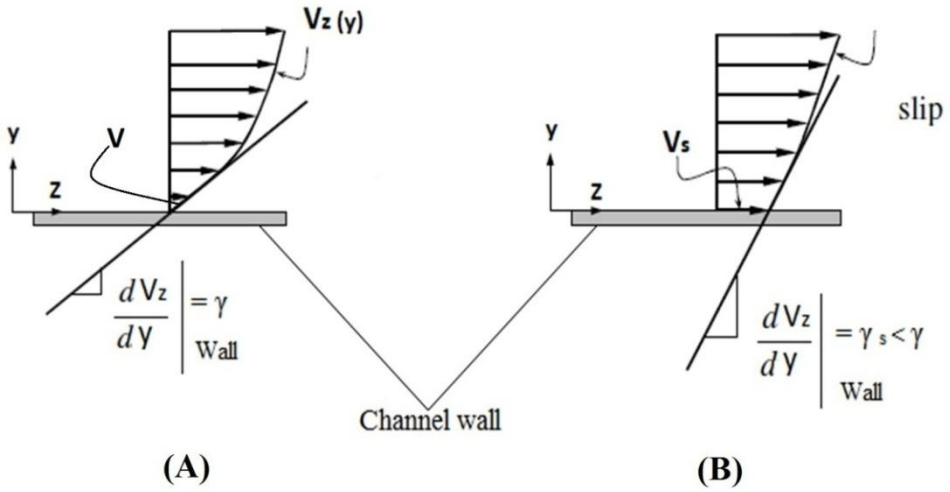

Figure 21: Mooney Analysis A) without slip B) with slip [36; 52]

Dissipative heating

Melt flow in a capillary leads to dissipative heating (due to friction), which is proportional to the local shear stress and the square of shear rate. Dissipative heating causes small changes in flow properties of plastic materials, hence, extra care should be taken to balance heat input to output. Therefore it is important to keep the temperature profile constant in a particular temperature range [56; 61].

2.5 RHEOLOGY OF PROTEIN BASED BIOPLASTICS

During the past few decades, efforts have been made around the world in the development of protein based bioplastics from renewable resources including plant and animal by-products. Proteins are natural polymers and are hard to process and convert into shaped articles. Improving processability is a challenge which requires an understanding of protein rheology.

The rheological behaviour of some common synthetic polymers is shown in Figure 22, to serve as a comparison to some protein based thermoplastics, discussed later.

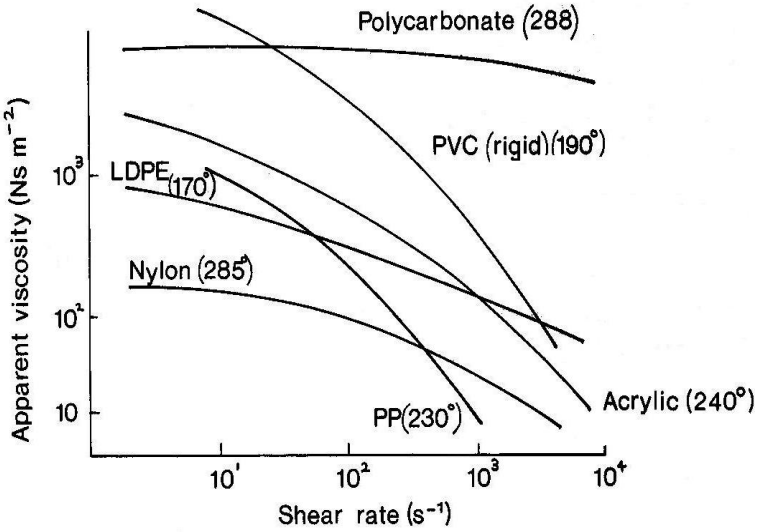

Figure 22: Apparent viscosity vs. shear rate for some common polymers [30]

2.5.1 Protein rheology and processing

Viscosity of soy protein plastics was determined using screw driven capillary rheometry [19]. In Figure 23 and Figure 24, the apparent viscosity is shown with respect to temperature and different additives. From these diagrams it can be observed that soy protein blended with corn starch exhibited shear thinning behaviour and the viscosity reduced with an increase in temperature. The material

showed similar behaviour for the different compositions tested, such as the addition of Na_2 So_3, and titanate. Soy protein without sodium sulfite (reducing agent) had comparatively higher viscosity than other compositions. The baseline composition had the lowest viscosity compared to high and low SPI to starch ratio blends. The compositions tested to analyse viscosity changes are listed in Table 4.

Table 4: Components of five different formulation of soy protein studied [19]

Batch label	Parts by weight (dry basis)		
	SPI:Corn starch	Sodium sulfite	Titanate
Baseline	1.5	1.4	0
High SPI:CS	4	1.4	0
Low SPI:CS	0.667	1.4	0
No Na_2 So_3	1.5	0	0
Titanate	1.5	1.4	0.3

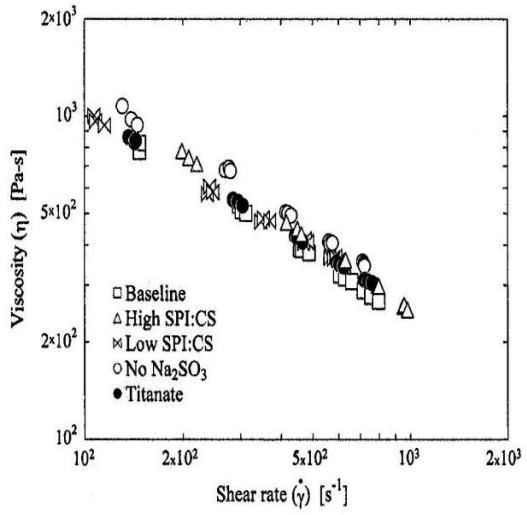

Figure 23: Comparison of soy protein viscosity with other material [19]

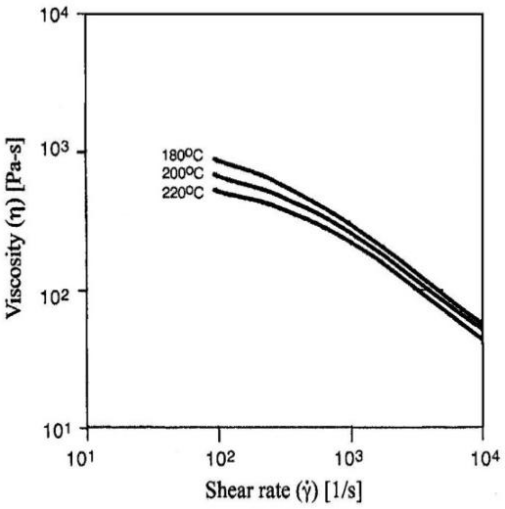

Figure 24: Viscosity of soy protein plastic and at different temperatures [19]

In another study, the rheological behaviour of gluten based bioplastics was determined using torque rheometry. The amount of water absorption by the protein depended on the nature of plasticisers and operating conditions. It was

shown that gluten bioplastics exhibited linear-visco-elastic behaviour when prepared by compression moulding. It was found that temperature greatly affected flowability and mechanical properties of the material [62]. Since proteins absorb water which leads to lower mechanical and physical properties after processing, it was found that choosing a appropriate plasticiser was important to reduce water content which may improve their mechanical properties during and after processing.

Rheology of whey protein isolated (WPI) and modified pectin complexes were determined by controlled strain rheometry [39]. Shear thinning behaviour was observed and a clear influence of particle size on rheology of samples during steady shear analysis was noticed, with the suspensions composed of the smaller diameter particles having the highest viscosity (Figure 25). It was also shown that altering the pH of the system will alter the flow properties [21].

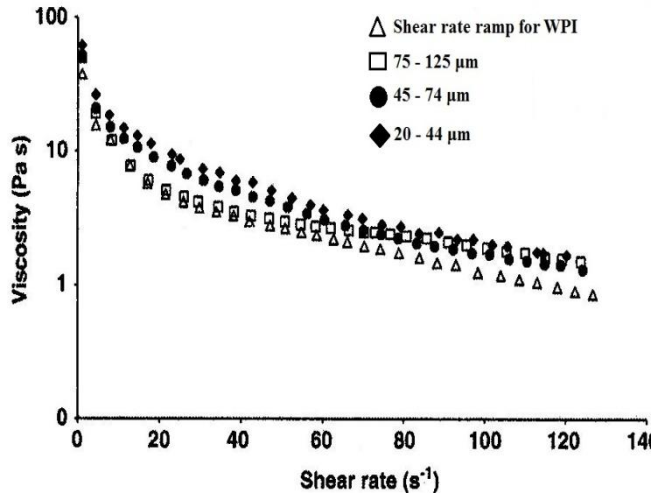

Figure 25: Viscosity of WPI with different particle sizes [21]

A rheomax single screw extruder equipped with a capillary die with L/D ratio of 10 and a diameter of 10 mm was used to measure the viscosity of sunflower protein isolate (SFPI). Trials were conducted at two different die temperatures.

The screw speed (RPM) ranged from 20 to 200 and the resulted shear rate was between 20- 150 s^{-1} [27]. In Figure 26 viscosity changes of SFPI with respect to temperature are shown.

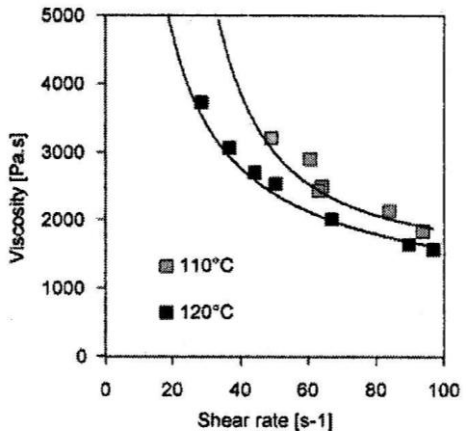

Figure 26: Apparent Viscosity vs. Shear rate for Sunflower Protein Isolate [27]

The effect moisture content, plasticiser content, temperature and addition of a reducing agent on the rheological behaviour of SFPI were investigated. Figure 27 shows the rheological behaviour of SFPI/glycerol/water mixtures at different ratios. It was shown that SFPI exhibited thermoplastic behaviour and is suitable for convention manufacturing processes, like injection moulding and extrusion [27]. Higher glycerol and water content had relatively lower viscosity and higher temperature reduced the viscosity of the polymer system.

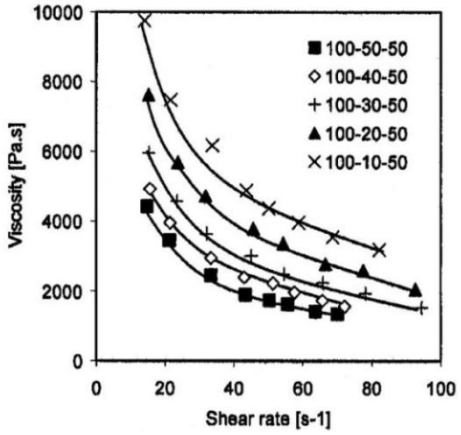

Figure 27: Effect of plasticisers (SFPI/glycerol/water) [27]

A study on rheology of soy protein blends used a Haake torque rheometry and high pressure capillary rheometry for viscosity measurement. The flowability of the soy protein was found to increase greatly when blended with poly (butylene succinate). Enhanced compatibility facilitated flow behaviour of soy protein. It was said that stronger molecular interaction should lead to better processability [9]. In Figure 28, viscosities at various temperatures for soy protein isolate (SPI) and soy protein isolate/poly (bultylene) succinate (SPI/PBS) are shown.

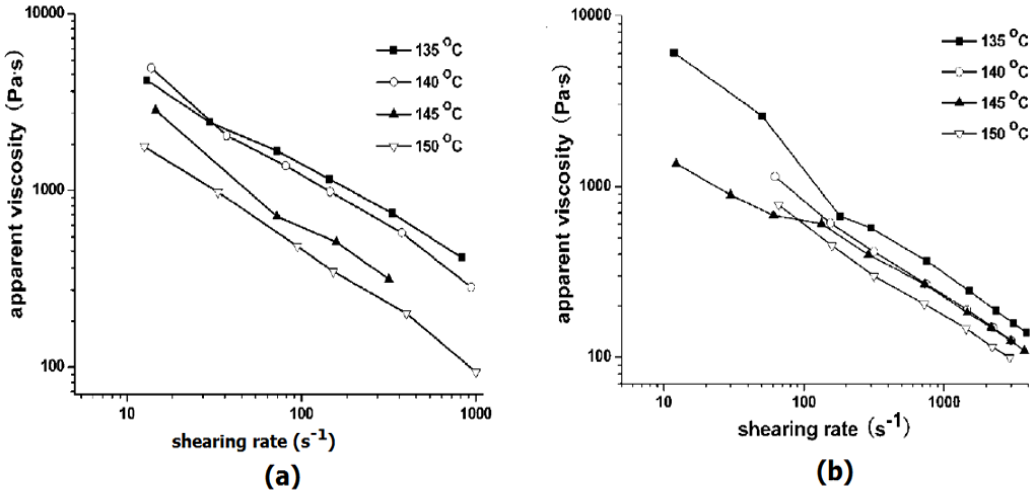

Figure 28: Effect of temperature on (a) SPI (b) SPI/PBS [28]

Rheological measurements of oats protein isolate were carried out by using stain-controlled fluid rheometry. This study was conducted in an enclosed chamber to avoid moisture loss. The measurement was based on storage modulus and loss modulus, since the loss modulus represents the dissipative component of mechanical properties and is characteristic of viscous flow. The shear rate ranged from 0.01 to 300 s^{-1}. Prior to rheological experiments, the material was subjected to different chemical processes such as acetylation and succinylaion and viscosity changes had been analysed.

It was found that the material displayed viscoelastic behaviour (non-linear and shear thinning) as all moduli curves exhibited a plateau at higher frequency. Figure 29 shows viscoelastic behaviour of a) 20% suspension of acetylated oat protein crosslinked with transglutaminase, b) 20% suspension of acid precipitated oats protein and c) 20% suspension of succinylated oat protein. Crosslinking of oats protein isolate appeared to stiffen the backbone of the polymer, reduced their mobility and solubility, thus viscosity was higher. The effect of crosslinking varied when the material went through different chemical processes [28].

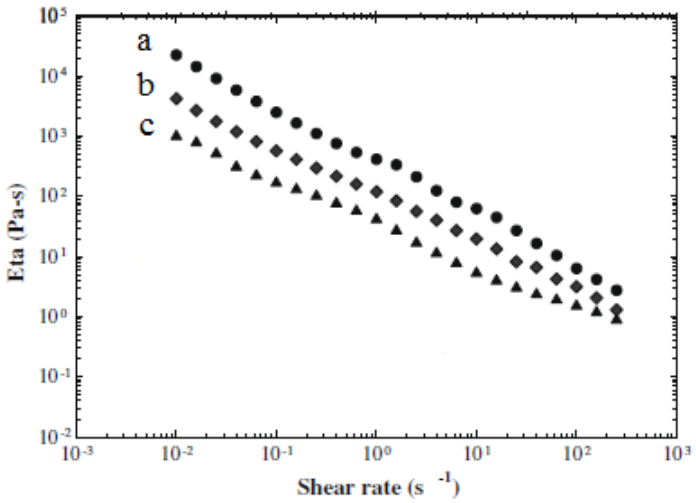

Figure 29: Non-linear steady shear viscosities for the 20% OPI suspension [28]

A summary of rheological studies for protein-based polymers are listed in the

Table 5.

Table 5: Summary of viscosity measurements for different proteins [16; 19; 22; 27; 62; 28; 64]

Author	Year	Material	Shear rate range (s^{-1})	Temperature range (°C)	Rheometry Type	Model	Correction
Hermansson	1975	SPI	0.01-1142	25	Co-Axial	Power law + yield stress	Not applicable
Jao, *et. al.*	1978	Soy flour	50-1000	100-160	Screw extrusion capillary	Power law	Bagley + Rabinowitsch
Luxen burg *et. al.*	1986	Defatted Soy flour	2-200	25-110	Piston extrusion capillary	Power + Exponential moisture	Large L/D so end effects neglected + Rabinowitsch
Battacharya *et. al.*	1989	CGM/SPC Blend	200-7400	145	Screw extrusion capillary	Power + Exponential moisture	Bagley + Rabinowitsch
Olivr *et. al.*	2003	Sunflower protein	1-150	100-150	Single screw extrusion capillary	Power law	Not applicable
Jerez *et. al.*	2005	Gluten plastic	10-1000	25-170	Torque rheometry	-	Not applicable
Daubert *et. al.*	2006	Whey protein	2-140	25	Stress Rheometry	-	Not applicable
Osswalt *et. al.*	2008	Soy protein	100-1500	170	Screw extrusion - capillary	Power law	Bagley + Rabinowitsch
Abdellatif *et. al.*	2009	Oats protein	0.001-1000	10-42	Strain controlled Cone-Cone	-	Not applicable

2.5.2 Effect of processing parameters on viscosity of polymers

Control of processing parameters is important to ensure a consistent product. The most important factors influencing the viscosity of polymers are: molecular mass, pressure, filler content, crosslinking, additives, plasticisers, moisture content and temperature [65]. The effect of these parameters are summarised in Figure 30.

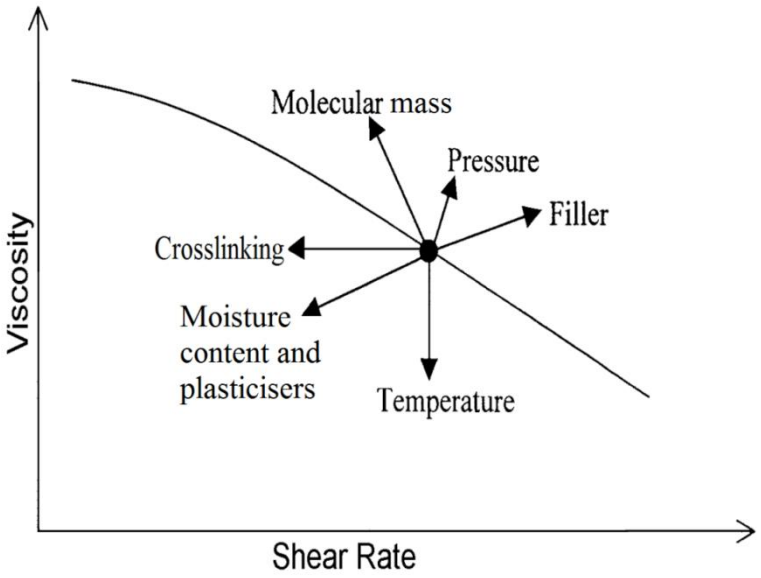

Figure 30: Influence of increasing various parameters on polymer viscosity [65]

Molecular mass

The molecular mass of a polymer is the most important factor affecting rheology. For most polymers the zero shear viscosity is approximately proportional to the mass-average-molecular mass of (M_m) below the critical molecular mass (M_c) and to the power 3.5 at molecular mass above M_c. (Equation 26 and 26a, Figure 31)

$$\eta = K_1 M_m \quad M_m < M_c$$
and (26)
$$\eta = K_2 M_m^{3.5} \quad M_m > M_c$$

A high molecular mass is required to attain good mechanical properties. The molecular mass distribution of a polymer also influences its rheology. In general,

a broader range leads to a lower shear rate at which shears thinning starts. Highly branched polymers also have higher viscosities [37; 46].

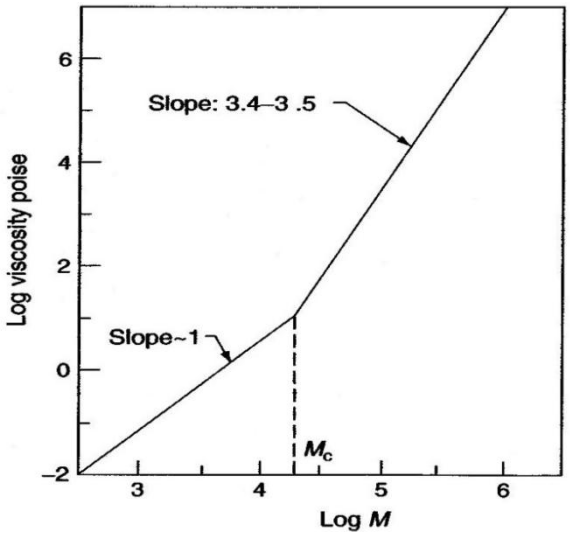

Figure 31: Dependence of polymer viscosity on molecular weight (M) [37]

Pressure

While temperature rises at constant pressure cause a decrease in viscosity, pressure rises at constant temperature cause an increase in viscosity, because of a decrease in free volume (free volume is defined as space between polymer molecules [5]). In other words, if the volume is kept constant by increasing pressure as temperature is increased, the viscosity also remains constant. It was found that within the normal processing temperature range for a polymer it is possible to consider an increase in pressure as equivalent, in its effect on viscosity, to a decrease in temperature [37].

Fillers

Fillers such carbon black, precipitated silica and calcium carbonates are usually added to the polymers during processing having some advantages such as cost reduction and control of density but it influences viscosity negatively, i.e. they

tend to increase viscosity of polymer systems as contrast to plasticisers [31]. A schematic representation of the effect of fillers is shown in Figure 32.

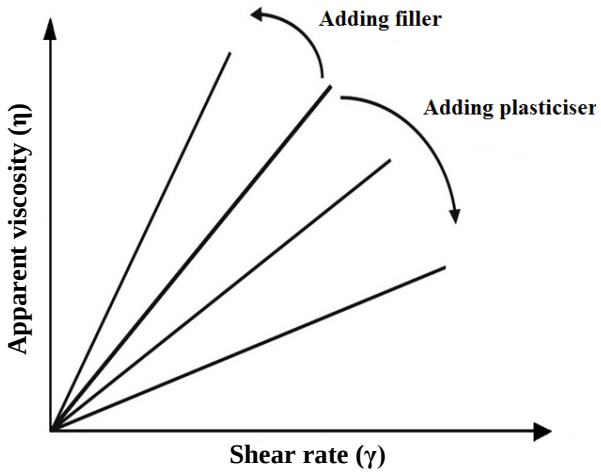

Figure 32: Effect of fillers and plasticisers on viscosity of polymers [66]

Crosslinking

The term crosslinking in polymers refers to inter and intra molecular covalent crosslinks between functional groups and restrain chain movement [5]. Formation of covalent crosslinks in proteins during extrusion may lead to increase in viscosity and changes in aggregation and solubility, making processing difficult. Furthermore, proteins containing lysine and cysteine amino acids may form additional crosslinks and it is necessary to control. Proteins, such as bloodmeal and feather keratin contain a large amount of cysteine and lysine [5]. These crosslinks can be controlled and cleaved by the addition of reducing agents such as sodium sulfite (Na_2 So_3).

Moisture content and plasticisers

Free volume of a polymer increases with increasing temperature, up to a point where it has enough space for movement. This point is called as glass transition, where large segments of the chain start moving [66]. The T_g signifies a major

transition for many polymers, as physical and mechanical properties change drastically as the material goes from a glassy to a rubbery state. T_g is useful to identify the degree of plasticisation in thermoplastics and also important in terms of viscosity measurements. Usually, the T_g must be low to for a polymer to have a low viscosity, thereby good flowability. T_g of a material can be analysed using different techniques such as, dynamic mechanical analysis (DMA), differential scanning calorimeter (DSC) and pulse thermal analysis (PTA) [7].

T_g of proteins varies based on protein source, moisture content and additives. Water has very low T_g of -135°C which makes it a effective plasticiser during extrusion. The effect of moisture content on some protein polymers is listed in Table 6 [6; 7; 67]. The effect of moisture content on viscosity is expressed in an extended Arrhenius equation (Equation 27).

To control or reduce T_g in polymers, plasticisers (e.g. glycerol) are added during processing [7]. Plasticisers are typically high boiling substances and are good solvents for polymers. The chemical structure of a plasticiser also influences its efficiency. Features such as polarity, hydrogen bonding capability and density will determine how it functions and make a polymer more processable. For protein polymers, water is a good plasticiser which greatly increases free volume, thereby reducing viscosity and also facilitating the action of other additives [5].

Table 6: Effect of moisture content on T_g for different protein polymers [7]

Protein source	Glass transition temperature at % water (°C)							Analysis technique
	0	5	10	15	20	25	30	
CGM	178	100	70	55	45	40	30	MDSC
Zein	139	70	40	10	<0	-	-	DSC
Casein	210	140	90	70	50	40	25	DMTA, PTA, DSC
Soya	172	105	80	60	45	35	35	DMA
Wheat gluten	162	110	65	40	20	18	<18	MDSC [31]

Another common group of plasticisers for proteins are polyols. Water and polyols do not interact with hydrophobic areas in protein chains which enhances the tendency to absorb water. Many studies have focussed on finding other plasticisers, but they were found to be incompatible with proteins [7].

Hydrophilic and Hydrophobicity

Proteins are hydrophilic and are therefore sensitive to water, that is, they tend to absorb water and can be water soluble. These terms have much to do with the structure of water (Figure 33). Water consists of two hydrogen atoms joined to one oxygen atom, all in a triangular pattern and it is polar. The oxygen is negatively charged whilst the hydrogen end is positively charged. Thus, water molecules are actually attracted to each other and form hydrogen bonds. Proteins contain variety of functional groups that can form hydrogen bonds with water and makes proteins highly hydrophilic [68; 69]. In addition, polyols such as triethylene glycol is also hydrophilic in nature, which makes proteins more water sensitive. The structure of TEG is shown in Figure 33.

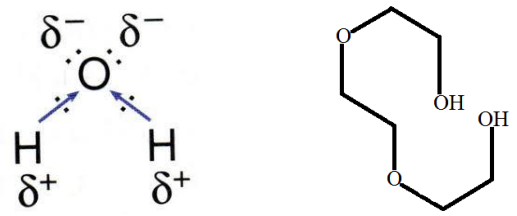

(A) **(B)**

Figure 33: Chemical structure of A) water [70] and B) TEG [71]

As a result, the mechanical properties and processability of protein polymers are highly dependent on water. On the other hand, materials such as polyethylene are hydrophobic and are insensitive to water, i.e. they would not absorb water and are insoluble in water [13].

Temperature

The viscoelasticity of polymers change with temperature; for protein polymers, temperature highly affects protein-protein interactions which will affect their viscosity [31]. As temperature increases, both rigidity and yield strength decrease, where as elongation generally increases, hence the mobility of the material increases [41].

An Arrhenius relationship (extended with moisture content, C_m) is often used to describe the temperature dependence of the viscosity of polymers:

$$\eta = k_1 \gamma^{n-1} \; e^{-k_2 T} \; e^{-k_3 C_m}$$

$$\ln(\eta) = (n-1)\ln(\gamma) + (\ln(k_1) - k_2 T - k_3 C_m) \qquad (27)$$

Where; k_1, k_2 and k_3 are constants, C_m is % moisture and T is temperature (in Kelvin) [19]. In Equation (27), when replacing (k_1-k_2T-k_3C_m) with ln K yields the standard power law model.

The WLF equation also explains why viscosity is more temperature sensitive with materials processed closer to their T_g. One interpretation of T_g is that it is a temperature below which the free volume is too small for significant molecular movement while above the T_g, molecules have sufficient energy for movement [37] (Figure 34).

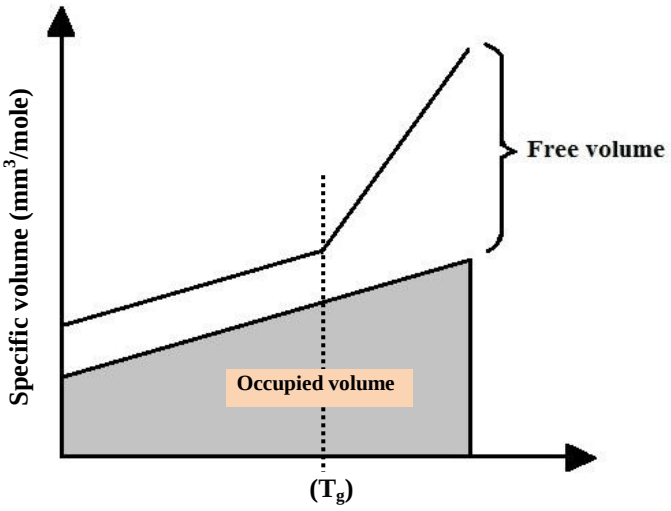

Figure 34: Free volume-temperature relationship [5]

Proteins are amorphous polymers and undergo a glass transition similar to synthetic polymers. In other words, a larger temperature gap between T_g and the operating temperature results in more the free volume available for movement [5].

$$\eta = \frac{-C_1(T-T_g)}{C_2 + (T-T_g)} \tag{28}$$

Where, C_1 and C_2 are material constants [36; 37; 41].

2.6 ASSESSING PROCESSABILITY

2.6.1 Batch mixing

Batch mixing is a process of mixing polymers by the action of shear in which they are consolidated and sometimes crosslinked. Batch mixers require a small quantity of material and give a preliminary testing analysis of a material.

Polymer, in powder form, is fed into the heated mixing chamber, in which it gets milled by two rotating kneaders at a fixed rotor speed. Torque is recorded as a function of time to monitor polymer viscosity. As the time progresses there is some volume shrinkage of the material at which torque increases due to steady-state consolidation, followed by crosslinking or degradation [9]. The following stages may occur during mixing (Figure 35):

i. When the polymer is introduced in the mixing chamber, the solid powder offers a certain resistance to the free rotation of the blades and therefore the torque increases.
ii. When the resistance is overcome, the torque required to rotate the blades at the fixed speed decreases and reaches a short steady state.
iii. The torque increases again due to the melting of the material.
iv. Consequently, the torque decreases and reaches a steady state region (v) and increases or decreases depending whether crosslinking or degradation takes place (vi) [9].

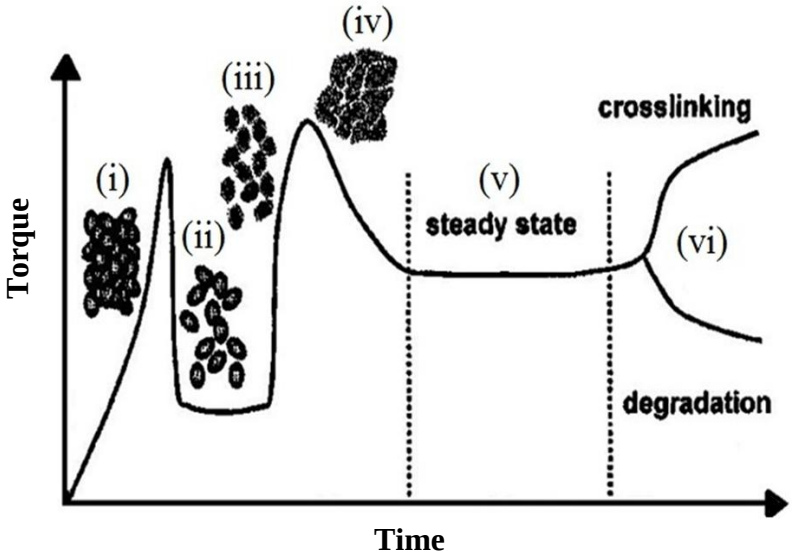

Figure 35: Typical variation of measured torque as a function of time [9]

2.6.2 Processing window

The processing window is the steady state interval between consolidation and crosslinking of a plastic material corresponding to the region (v) in Figure 35. During extrusion, a material should travel in the barrel for a particular time at a given temperature for the material to consolidate, but not crosslink. Once an appropriate window has been established it can be used for process design. The processing window can be predicted by the use of a batch mixer, by monitoring the time between consolidation and crosslinking as indicated by changes in torque.

The torque changes through time for gluten based bioplastic was characterised in a mixer chamber by monitoring the evolution of torque and temperature with time. Three regions were observed, as shown in Figure 36.

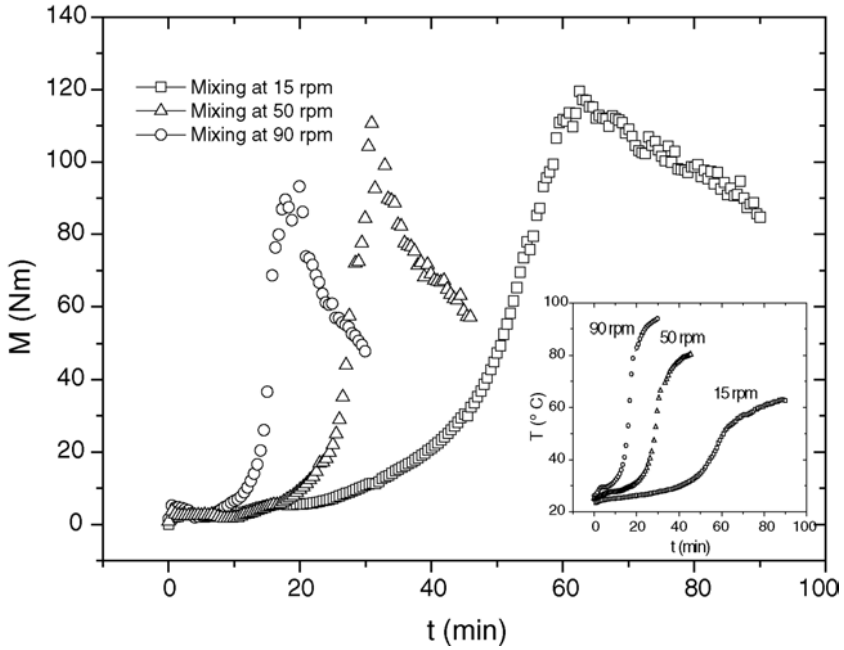

Figure 36: Torque changes in gluten bioplastic with respect to temperature and onset to consolidation [22]

In the first region, no increase in torque was observed and corresponded to an induction period. The length of the induction period decreased with increased mixing speed. In the second region, the torque increased to a maximum as the material consolidated. A sudden drop in torque was observed in the final region. The time to reach the peak torque decreased with temperature [22].

In a study of wheat gluten-based bioplastic blends, three torque regions were also observed during batch mixing (Figure 37) [62]. The three regions were similar to gluten bioplastic discussed earlier. The final decay of the torque was associated with plasticiser content. The maximum torque was reached faster when the plasticiser amount was reduced, while high water content increased the mixing time, and maximum torque was reached slower compared to other plasticisers [62].

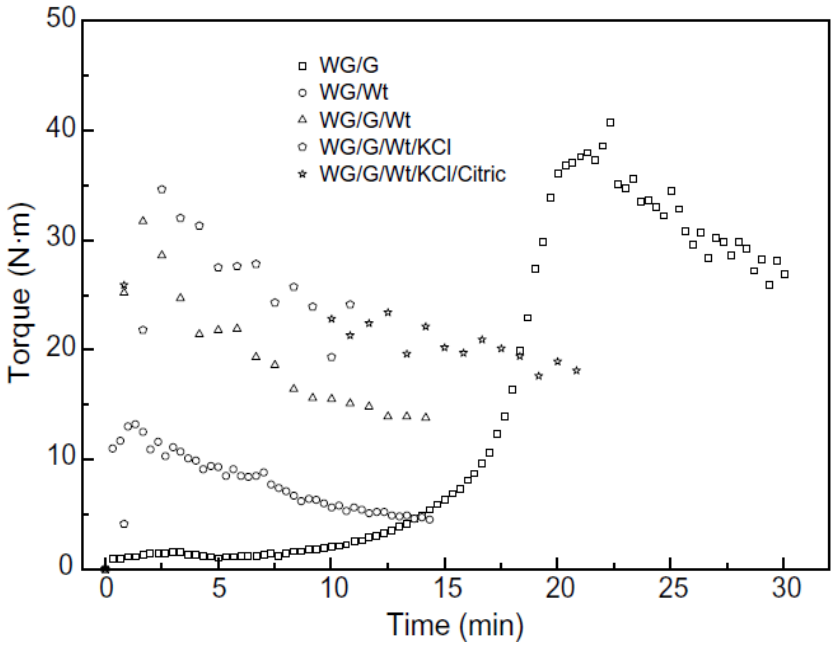

Figure 37: Evolution of torque during the mixing process of wheat gluten with different blends [62]

Plasticisation of wheat gluten with fatty acids in a counter rotating batch mixer enabled the assessment of the process window for that material [23]. The study showed possible plasticising effects through torque vs. mixing time and the results were supported by DSC measurements. It was found that torque increased faster at lower plasticiser content, higher temperature and shear. The time to reach the maximum, as a function of plasticiser content, increased exponentially at a given regulation temperature. In Figure 38, torque vs. time curves is shown for gluten plasticised with different fatty acids. It was shown that longer hydrocarbon chain fatty acids prolonged the processing window [23].

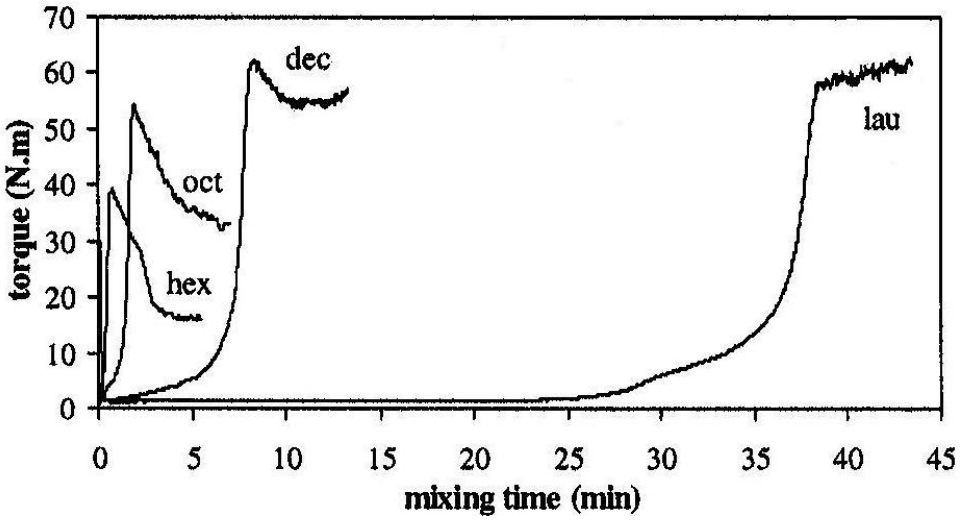

Figure 38: Torque evaluation of wheat gluten plastic with different fatty acid [23]

2.6.3 Rheology

A general torque vs. time analysis allows determination of shear rate and viscosity from batch mixing data [9]. For the purpose of analysis, the mixing elements could be represented by two concentric cylinders exerting the same torque as the mixing heads, as shown in Figure 39 and a couette analogy (a technique to illustrate dimensions) is shown in Figure 40 .

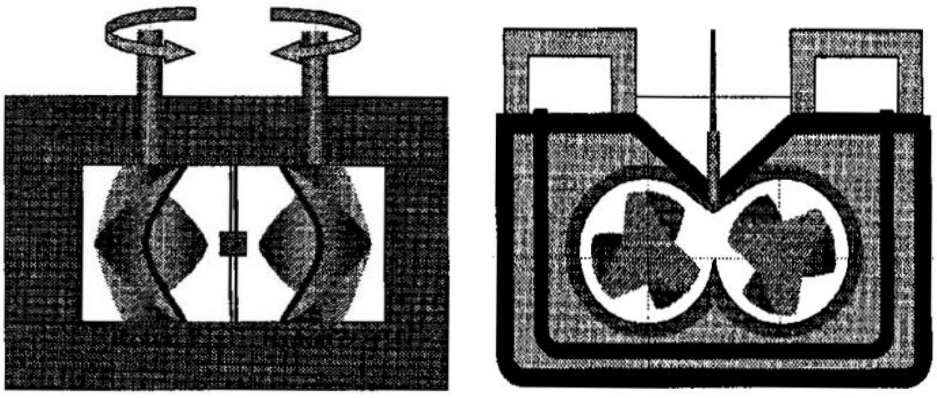

Front view Lateral view

Figure 39: Design of batch mixer [9]

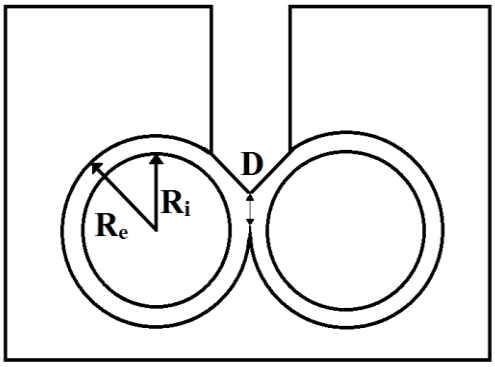

Couette Analogy

Figure 40: Schematic illustration of twin rotor batch mixer [9]

In the study of Bousmina *et al.* an effective internal radius (R_i) was determined for different polymers and processing conditions. It was found that R_i is a universal quantity practically insensitive to the nature and rheology behaviour of the melt. The concept was to convert torque-rotor speed data into viscosity and shear rate data. Fluid flow in the batch mixer was modelled by equivalent flow generated between two concentric cylinders rotating at constant speed, exerting same torque as batch mixer elements.

A calibration procedure was used to calculate the effective internal radius, using a polymer of which the power law constants are known and can be calculated using the following expression:

$$R_i = \frac{R_e}{\left[1+\frac{4\pi N}{n}\left(2\pi MLR_e^{2}\frac{1+G^{n+1}}{r}\right)^{\frac{1}{n}}\right]^{\frac{n}{2}}} \qquad (29)$$

The shear rate at the position, $(R_i - R_e)/ R_i$, is given by:

$$\text{Shear rate } (\gamma) = \gamma_{½} = \frac{(2^{2\left(1+\frac{1}{n}\right)}\,\pi\, N)}{n}\,\frac{\frac{\beta 2}{n}}{\frac{(1+\beta)2}{n}\left(\frac{\beta 2}{n}-1\right)}\ (s^{-1}) \qquad (30)$$

$$\text{Shear stress } (\tau) = \tau_{½} = \frac{2}{\pi L \beta^2 (1+Gn+1)} \text{ (Pa)} \quad (31)$$

$$\text{Viscosity } (\eta) = \frac{2r}{\pi L \beta^2 (1+Gn+1)} \text{ (Pa.s)} \quad (32)$$

Where;

$\beta \rightarrow (R_e/R_i)$

$R_e \rightarrow$ External cylinder radius (mm)

$R_i \rightarrow$ Internal cylinder radius (mm)

M→ Polymer melt consistency

N→ Speed of cylinder rotation

n→ Flow behaviour index (from Power law)

L→ Length of the cylinder (mm)

G→ Gear ratio between two rotors

Γ→ Torque obtained from batch mixer (Nm)

$(R_{1/2}) \rightarrow r = (R_e/R_i)/2$

In these expressions the torque is measured in the steady state region, as indicated by Figure 35.

Viscosity data from batch mixing was found to be in reasonable agreement with the data obtained from capillary rheometry as shown in Figure 41 [9].

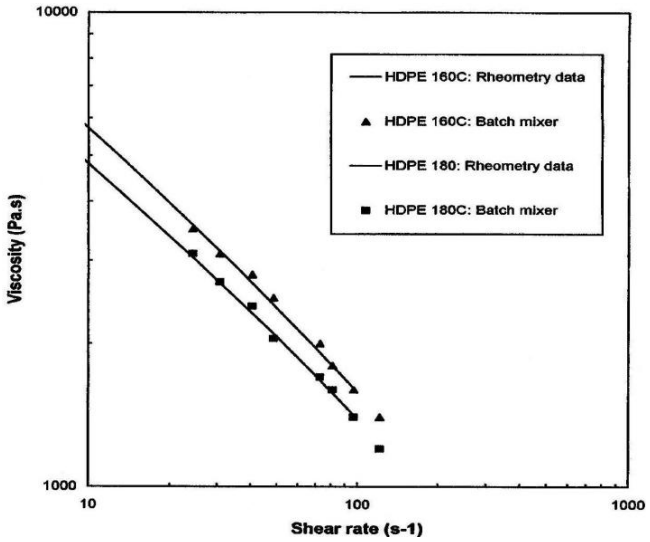

Figure 41: Comparison of viscosity data of HDPE measured using capillary rheometry and batch mixing [9]

In summary, batch mixer data can be useful to identify the processing window which will be useful to assess processability of protein-based plastics. The effects of temperature and shear as well as the addition of plasticisers are important parameters and strongly influence the obtainable processing window.

2.7 NOVATEIN THERMOPLASTIC PROTEIN (NTP)

Due to advances in protein polymer engineering, bovine blood is used as a source to produce biodegradable bloodmeal plastics. Bloodmeal is a reddish-brown powder derived from bovine blood after drying. Raw blood contains about ~80% water and ~18% protein [6]. The chemical composition of commercial bloodmeal is listed in Table 7 [72].

Table 7: Chemical composition of blood meal (wt% in dry matter) [72]

Component	Bloodmeal	
	Mean	**Variation**
Organic matter	92.9	73. 8 - 97.8
Crude protein	92.5	72.3 - 96.6
N-free extracts	3.3	0 - 10.7
Crude fat	1.2	0 - 5.9
Crude ash	5.3	2.0 - 15.6

2.7.1 Bloodmeal production

Soon after collection, blood tend to coagulate (coagulation is the formation of insoluble complexes in proteins). To restrain coagulation, anticoagulants (e.g. oxalic acid) are added to blood. Coagulation affects thermal and oxidative (putrefactive deterioration) degradation of proteins. To avoid putrefaction during transportation, formic acid, sodium chloride, unslaked lime and 3% sulphuric acid are added to blood during collection [73].

There are many ways to produce bloodmeal: commonly, before dewatering, whole blood is filtered to remove fragments and coagulated using stream injection at 90°C [74]. The coagulant is separated using a centrifuge. The coagulant is dried in a rotating drum at the temperature between 120°C and 175°C to a final moisture content of 2-4 wt%. After drying, bloodmeal is powdered a using hammer mill [73; 74].

2.7.2 Processing of NTP

NTP is prepared from bloodmeal using water, sodium dodecyl sulfate (SDS), sodium sulfite (SS) and triethylene glycol (TEG). Additives are primarily used to ensure sufficient inter and intra molecular interactions between polymer chains.

Water

Water is required for processing mainly to facilitate the action of additives and ensures uniform dispersion of additives in bloodmeal. It also acts as a plasticiser and reduces the denaturing temperature of the proteins [6].

Sodium Sulfite

Sodium sulfite is a reducing agent which is mainly used to break disulfide crosslinks. These crosslinks are heat resistant and prevent the formation of a flowable melt [6].

Urea

Water molecules surround protein chains in their native state ad may protect it from denaturation. Urea preferentially binds to the protein surface, disrupting the interaction between proteins and water, resulting in partially unfolded and flexible protein chains. The denatured protein may form entanglements and crosslinks during the moulding process, resulting in plastics with a high tensile strength, greater elongation and reduced water absorption [6].

Sodium Dodecyl Sulfate (SDS)

SDS is an anionic detergent known to produce considerable conformational changes in proteins at concentrations in the order of 0.02 mol/L. SDS does not

cleave disulfide bonds, but prevents hydrophobic and electrostatic interactions between protein chains, leading to an ordered denatured state [6; 75].

Triethylene Glycol (TEG)

Plasticisers are needed in polymer processing for effective processing. Plasticisers improve processability by interposing itself between polymer chains and alter the forces holding chains together [7].

Novatein Thermoplastic Protein (NTP) is extruded and granulated for further processing, such as injection moulding or compression moulding. In Figure 42, NTP is shown at its various stages of production; A) after synthesis B) extrusion C) granulation D) injection moulding respectively.

(A) **(B)** **(C)** **(D)**

Figure 42: Bloodmeal (NTP)

CHAPTER 3: EXPERIMENTAL

3.1 MATERIALS

The materials used in the preparation of NTP are shown in Table 8.

Table 8: Chemicals needed for formulation of NTP [7]

Chemical	Supplier	Grade
Bloodmeal (BM)	Wallace Corporation	ρ= 1300 kg/m^3
Sodium dodecyl sulphate (SDS)	Bio lab	Technical
Sodium sulphite (SS)	BDH lab Supplies	Analytical
Tri Ethylene Glycol (TEG)	Sigma Aldrich	Technical
Urea	Balance Agrinutrients	Agricultural
LLDPE	Borstar- FB2310	ρ= 931 kg/m^3 MFI= 0.9 g/10 min
Distilled water	Laboratory use	

3.1.1 Equipment

Extruder and capillary rheometry

All experiments were carried out using a twin screw extruder (TSE 16 TC 25:1), shown in Figure 43, with specifications listed in Table 9. The extruder was equipped with a capillary die for rheological measurements and it was connected with cooling system to control barrel temperature (Figure 44). The capillary had an inside diameter of 2.88 and length of 24.57 mm (L/D = 8.54).

Figure 43: Extruder setup

Figure 44: Capillary setup

In Figure 45, the screw design is shown as well as the temperature profile used for extrusion. The temperature of the die was varied according to the experimental plan followed.

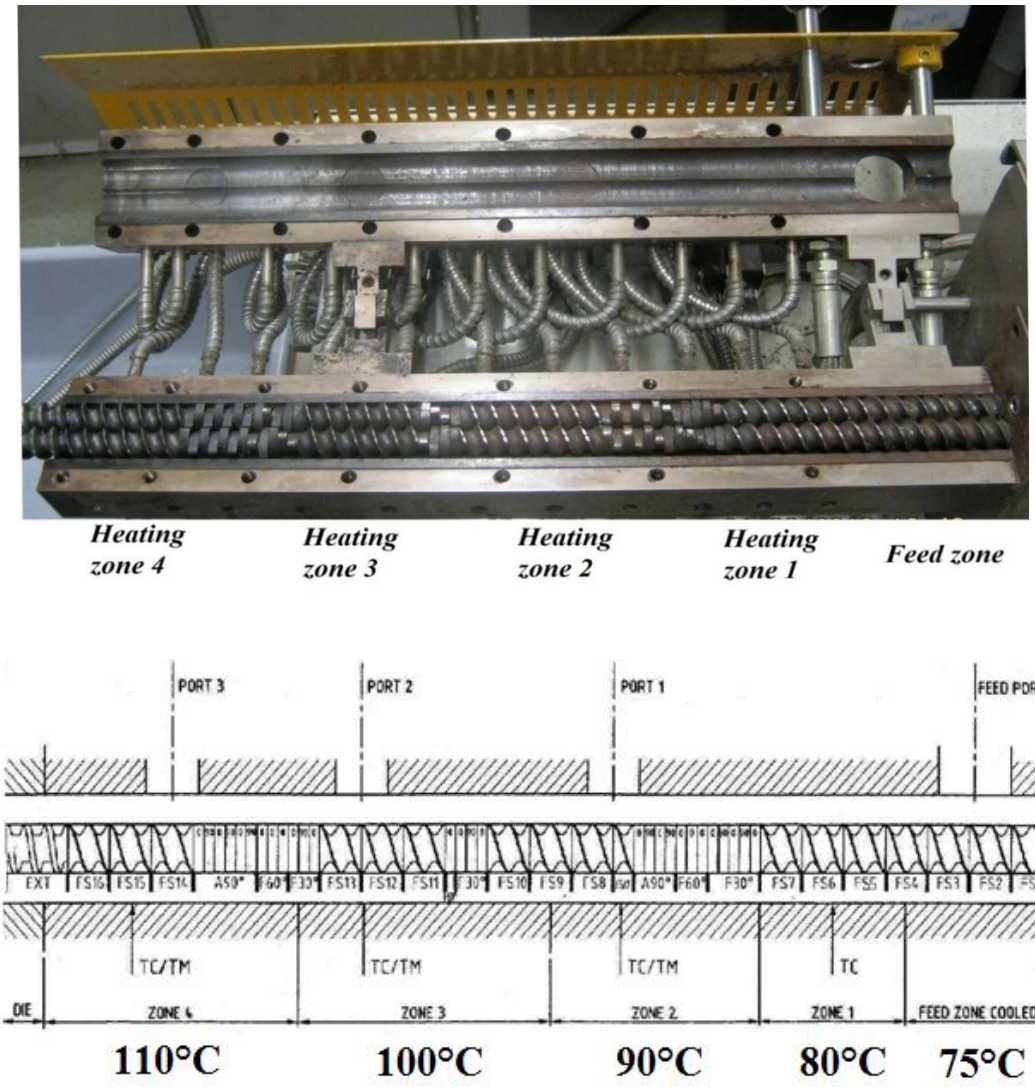

Figure 45: Extruder temperature profile and screw configuration

Table 9: Specification of the extruder used

Term	Specification	Term	Specification
Twin Bore (Ø)	16mm	Max Operating pressure	100 Bar
Screw (Ø)	15.60mm	Pressure Transducer	200 Bar
Channel Depth	3.30mm	Centres/Radius Ratio	1.5625
Die Length	16mm (1D)	Temperature Control	3 Term P.I.D Control
Barrel Length	384mm (24D)	Barrel Heating	D.C. Thyristor
Max Screw Speed	500 RPM	Overall Enclosure rating	I.P.44

Material was fed through a feeder (Hunter- Screw driven feed mechanism), which was capable of vary feed rate from 10 g to 100 g per minute. The feeder is shown in Figure 46.

Figure 46: Feeder with control

Batch Mixer

A batch mixer was modified to provide the required experimental data. An ordinary batch mixer was equipped with a Kistler Torque Sensor. This allowed torque to be recovered as a function of time. The batch mixer configured of two counter-rotating shafts with a turning ratio of 3:1 (Figure 47). A top view of the batch mixer is shown in Figure 48. The complete setup is shown in Figure 49.

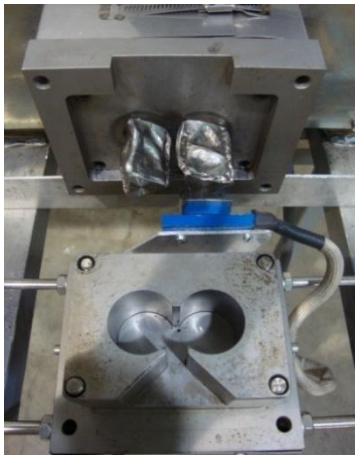

Figure 47 : Batch mixer head

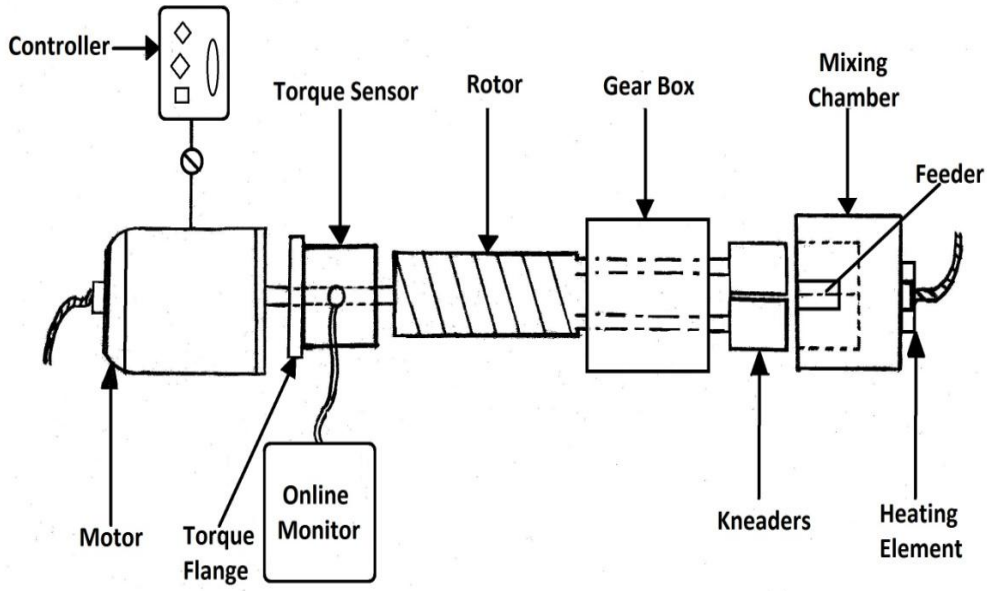

Figure 48: Top view of batch mixer

Figure 49: Batch mixer equipped with torque sensor

Dynamic Mechanical Analyser (DMA)

NTP was scanned through Dynamic Mechanical Analysis (DMA) to relate the rheological characteristics obtained by both capillary and batch mixer.

A Perkin Elmer dynamic mechanical analyser (Model DMA 8000- shown in Figure 50) with rotating analysis head (both vertical and horizontal) was used to

analyse dynamic properties of NTP. A powder pocket method was used, where powder material is analysed in a metal envelope that is several orders of magnitude stiffer than the test sample. This allows evaluation of the polymer's thermal properties, as described by the ratio of the loss modulus (E") and storage modulus (E') or $\tan(\delta) = \frac{E\prime}{E''}$. In powder pocket analysis, only $\tan(\delta)$ is of relevance, since the measured moduli would incorporate that of the pocket material. A frequency of 1 Hz was used and temperature ranged from room temperature to 250°C. Samples were tested using a single cantilever clamp and at a maximum strain of 0.002.

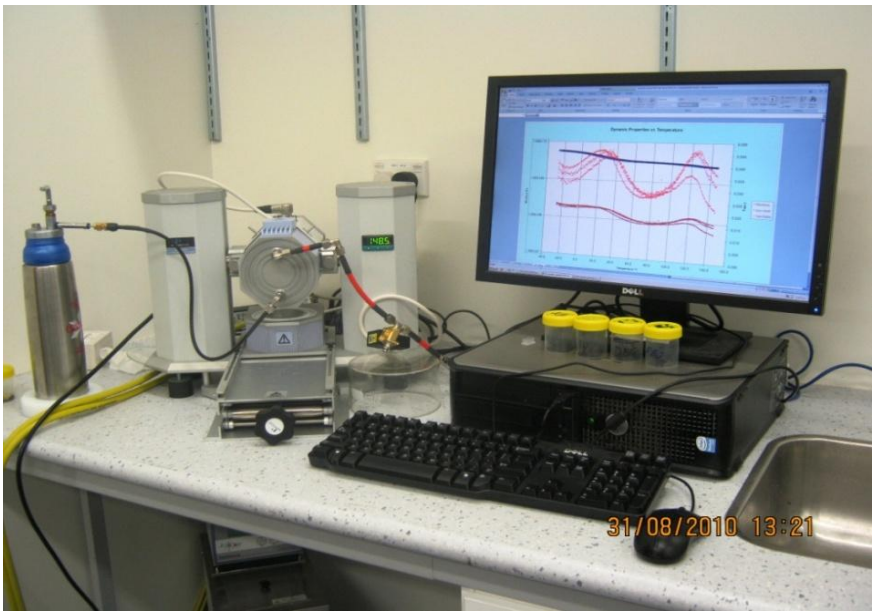

Figure 50: Dynamic Mechanical Analyser

3.2 METHODS AND EXPERIMENTAL DESIGN

3.2.1 Preparation of NTP

Standard NTP was prepared according to the method shown in Figure 51. The required amounts of urea, sodium sulfite (SS) and sodium dodecyl sulphate (SDS) were dissolved in water and heated to 60°C. The solution was mixed with

bloodmeal in a high speed mixer until the protein has absorbed all the water. Following denaturing, plasticiser (TEG) was added and the mixture was homogenised prior to extrusion.

In Table 10, the standard formulation is shown as well as the three other formulations used in this study. In formulations 1, 2 and 3, the total amount of plasticiser (water + TEG) was kept constant, but the ratio between water and TEG was varied.

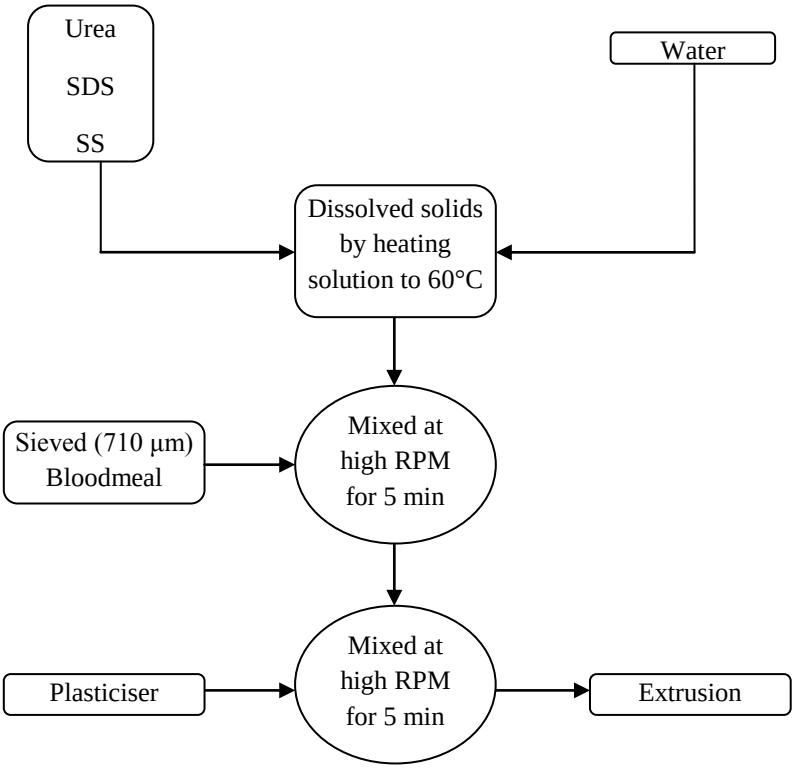

Figure 51: Basic preparation of NTP [76]

Table 10: Ratio of chemicals used for experiments

Material	Parts per hundred parts bloodmeal (pph_{BM})			
	Standard	**Formulation 1**	**Formulation 2**	**Formulation 3**
Sodium Sulfite	3	3	3	3
Sodium dodecyl sulfate	3	3	3	3
Urea	10	10	10	10
Triethylene glycol	10	10	20	30
Water	60	50	40	30

3.2.2 Capillary Rheometry

The effect of three different ratios of water:TEG on the rheology of NTP at three different die temperatures. Table 11 shows the experimental design.

Table 11: Capillary rheometry experimental design

Die temperature / Formulation	**115°C**	**120°C**	**125°C**
Standard	Exp. 1	Exp. 2	Exp. 3
Formulation 1 (Water 50: TEG 10)	Exp. 4	Exp. 5	Exp. 6
Formulation 2 (Water 40: TEG 20)	Exp. 7	Exp. 8	Exp. 9
Formulation 3 (Water 30: TEG 30)	Exp. 10	Exp. 11	Exp. 12

Method

1. The extruder die was equipped with a capillary die, pressure transducer and a temperature sensor.
2. The experimental temperature was set, and the equipment was allowed to equilibrate.
3. The material was extruded through a capillary at a set screw speed.
4. Mass flow rate was controlled by adjusting screw speed and feed rate of the extruder.
5. The volumetric flow rate (Q) was calculated by weighing material collected over 2 minutes. A constant density of 0.85 g/cm^3 was assumed.
6. The pressure at the capillary inlet was recorded for each selected screw speed. RPM was increased stepwise from 25 to 250 in increments of 25.
7. The temperature of capillary was periodically monitored using a thermocouple.
8. The torque was maintained between 40 and 50 Nm by adjusting the material feed to the extruder.
9. Each experiment was repeated in triplicate.
10. From pressure drop and volumetric flow rate the required rheological data could be calculated using Equations (16), (17) and (18).

3.2.3 Batch mixer

The processing window of the same four NTP formulations was assessed using a batch mixer. The process window is defined as the time it takes for the formulation to crosslink. The effect of temperature and shear rate (RPM) on processability was investigated according to the outline in

Table 12.

Method

1. Before each experiment, the mixing head and kneaders were cleaned to avoid cross contamination.
2. The required temperature was selected and the equipment was allowed to equilibrate.
3. The mixing chamber was filled with 65 g of NPT, which corresponded to about 85% of the mixing chamber's volume to allow for effective distribution of the material.
4. Mixing proceeded until the material crosslinked, as evident from a sudden rise in torque.
5. Each experiment was done in triplicate and average was taken for analysis.

Analysis

In Figure 52, a typical torque vs. time graph is shown. Form these graphs, the time to reach crosslinking (t_{max}) and maximum torque (Γ_{max}) can be obtained. The onset

to consolidation (t_r) was taken as the intercept of the tangents to each section of the torque vs. time graph as shown in

Figure 52. Δt represents the processing window and is defined as the time from the onset to consolidation to crosslinking ($\Delta t = t_{max}-t_r$).

Results were analysed by fitting a moving average trend line to the recorded data. The onset to consolidation (t_r) and time to maximum torque (t_{max}) were measured using the fitted curve.

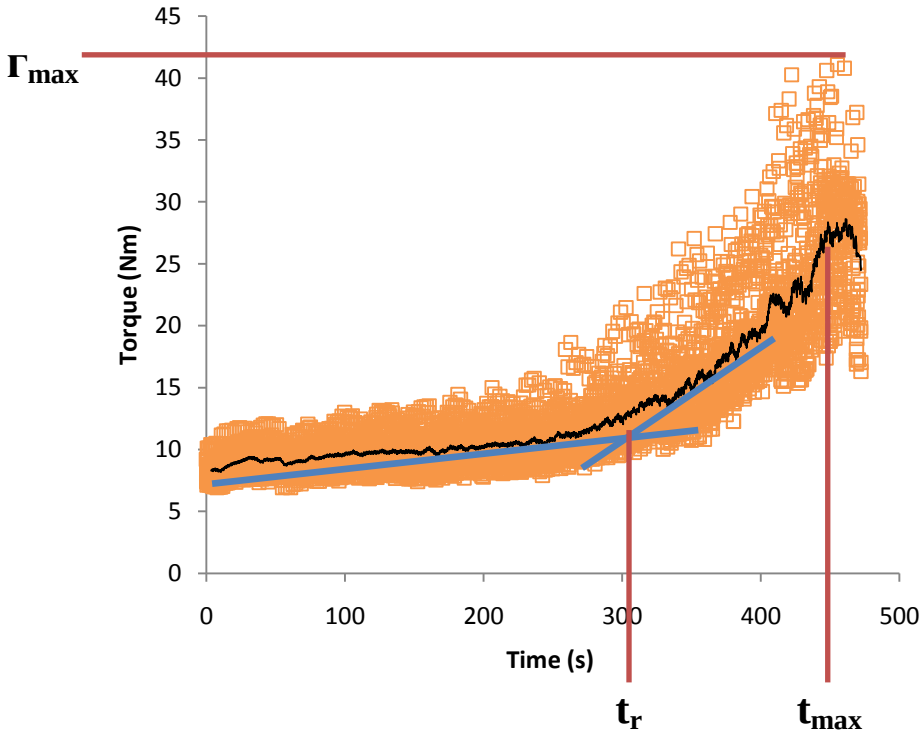

Figure 52: Data analysis technique for batch mixer results

Table 12: Batch mixer experimental design

Die temperature / Formulation	115°C				120°C				125°C			
	RPM 50	RPM 75	RPM 85	RPM 95	RPM 50	RPM 75	RPM 85	RPM 95	RPM 50	RPM 75	RPM 85	RPM 95
Standard	Exp.1	Exp.2	Exp.3	Exp.4	Exp.5	Exp.6	Exp.7	Exp.8	Exp.9	Exp.10	Exp.11	Exp.12
Formulation 1 (Water 50: TEG 10)	Exp.13	Exp.14	Exp.15	Exp.16	Exp.17	Exp.18	Exp.19	Exp.20	Exp.21	Exp.22	Exp.23	Exp.24
Formulation 2 (Water 40: TEG 20)	Exp.25	Exp.26	Exp.27	Exp.28	Exp.29	Exp.30	Exp.31	Exp.32	Exp.33	Exp.34	Exp.35	Exp.36
Formulation 3 (Water 30: TEG 30)	Exp.37	Exp.38	Exp.39	Exp.40	Exp.41	Exp.42	Exp.43	Exp.44	Exp.45	Exp.46	Exp.47	Exp.48

CHAPTER 4: RESULTS AND DISSCUSSION

In this chapter, the rheology of NTP was analysed using results obtained from capillary and batch mixer experiments. Analysis was based on the effect of temperature and water to plasticiser ratio.

Proteins are hydrophilic in nature and tend to absorb water which affects their physical and mechanical properties when they are converted into usable polymer products. In addition, water is generally used as a plasticiser in proteins during extrusion, but water loss after extrusion leads to a reduction in mechanical properties. Reducing the amount of water may lead to processing difficulties, but could be offset by using other plasticisers.

Viscosity of LLDPE

In Figure 53, the apparent viscosity ($\eta_{apparent}$) vs. shear rate (γ) for linear low density polyethylene (LLDPE) is shown. The material was tested at three different die temperatures (130 °C, 135 °C and 140 °C). The material flowed continuously and homogenously in the extruder barrel as well as the capillary. As expected, LLDPE showed non-Newtonian, shear thinning behaviour and the viscosity decreased with an increase in temperature. It was found that the rheology could be modelled as a power law fluid, for which the constants are shown in Table 13.

Table 13: Power law constants for LLDPE

Temperature (°C)	Flow behaviour index (n) (Dimensionless)	K (Pa.s)
130	0.34	5568
135	0.36	4350
140	0.44	2977

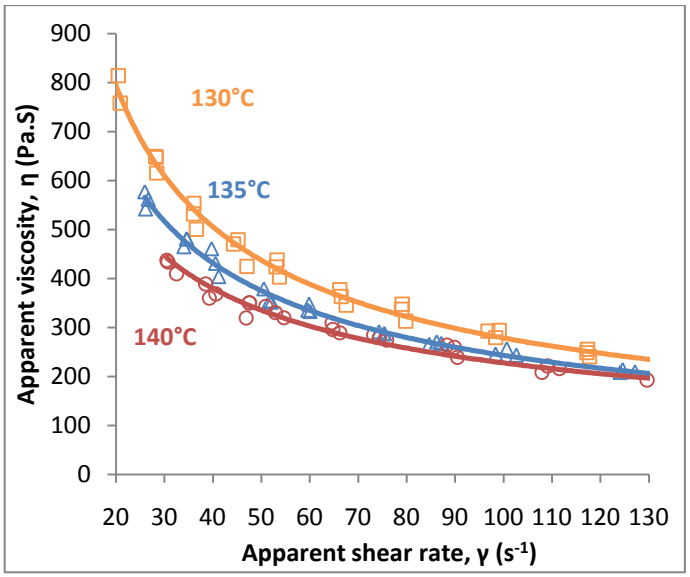

Figure 53: Apparent viscosity vs. shear rate for LLDPE [at 130°C, 135 °C and 140 °C]

The results obtained here, was also compared to published data for blends of LLDPE and LDPE (Figure 54 and Figure 56) with melt flow index (MFI) of 1 and 4 g/10min respectively [77]. (LLDPE used in this study had a MFI of 0.9 g/10min). The observed apparent viscosity in this study was very similar to that shown in Figure 54.

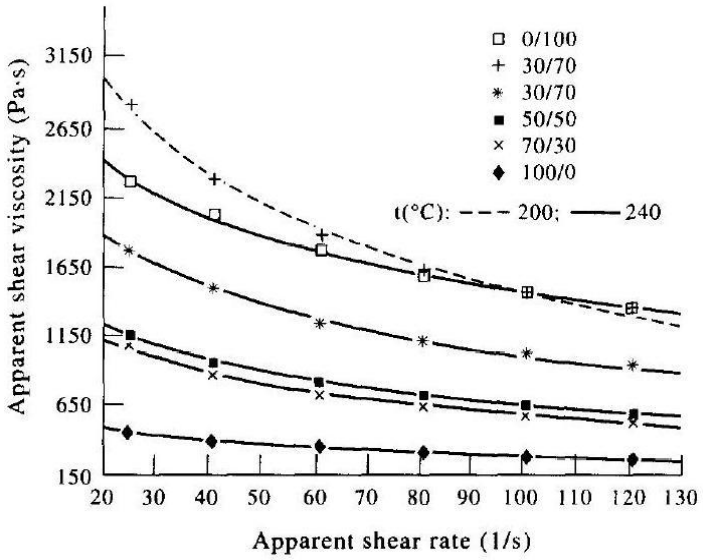

Figure 54: Apparent viscosity vs. shear rate for LLDPE/LDPE blends [77]

A discontinuity in a shear rate vs. shear stress curve is commonly used to identify the existence of melt fracture or wall slip. Melt fracture did not occur during LLDPE processing, suggesting continuous melt flow, without disturbance over the range of shear rates studied (Figure 55).

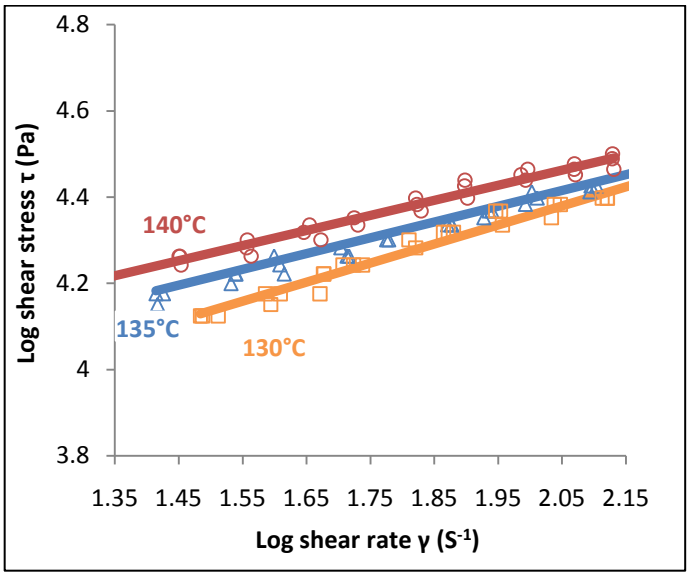

Figure 55: Log shear rate vs. log shear stress for LLDPE [at 130°C, 135 °C and 140 °C]

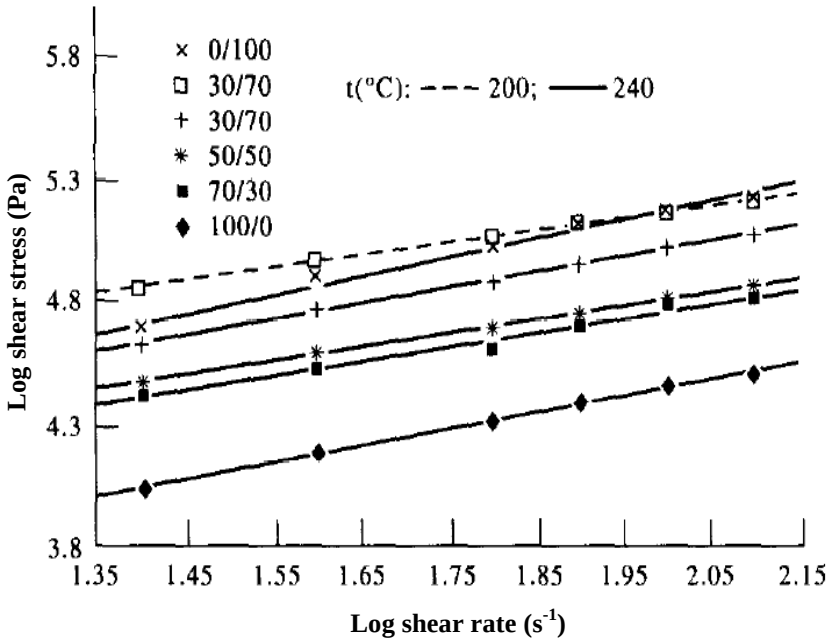

Figure 56: Log shear rate vs. log shear stress LDPE/LLDPE blends at different ratios [77]

Based on these results, it was concluded that the experimental setup was appropriate and was consistent with that observed from literature. The same conditions were used to compare the various NTP formulations, using LLDPE at 130°C as a reference.

4.1 RHEOLOGY OF NTP

The apparent viscosity vs. shear rate curves for the various formulations tested are shown in Figure 57, Figure 58 and Figure 59. It can be seen that NTP displayed non-Newtonian, shear thinning behaviour at all the temperatures tested. The rheology of NTP is similar to other thermoplastic proteins, such as soy protein [29] and sunflower protein isolate [42] (see section 2.5.1).

From these figures, it can be observed that the viscosity of NTP is considerably higher than that of LLDPE, especially at low shear rates. It does, however, follow similar shear thinning behaviour.

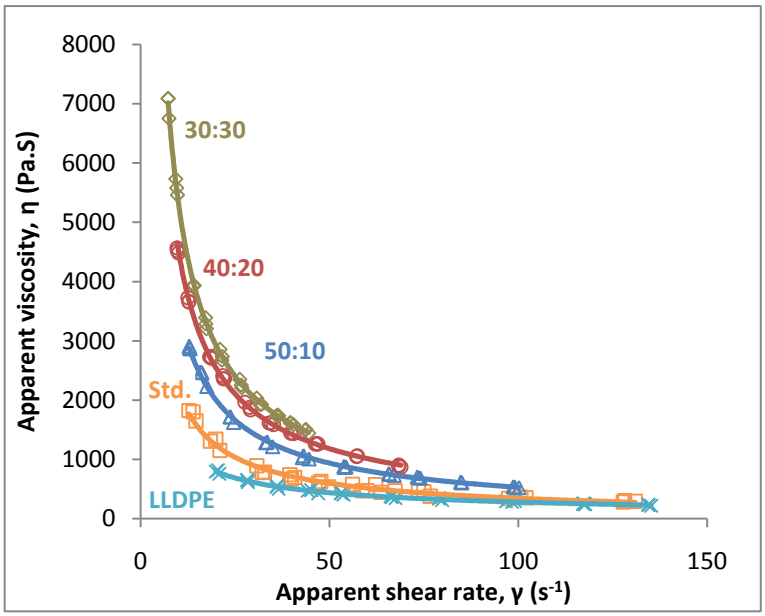

Figure 57: Apparent viscosity vs. shear rate for four different formulations [Std., 50:10, 40:20, 30:30 & LLDPE] at 115°C

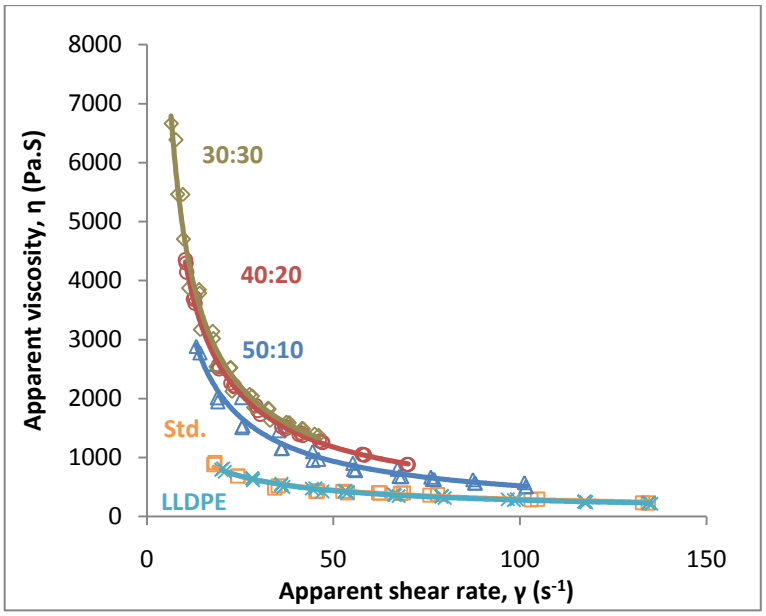

Figure 58: Apparent viscosity vs. shear rate for four different formulations [Std., 50:10, 40:20, 30:30 & LLDPE] at 120°C

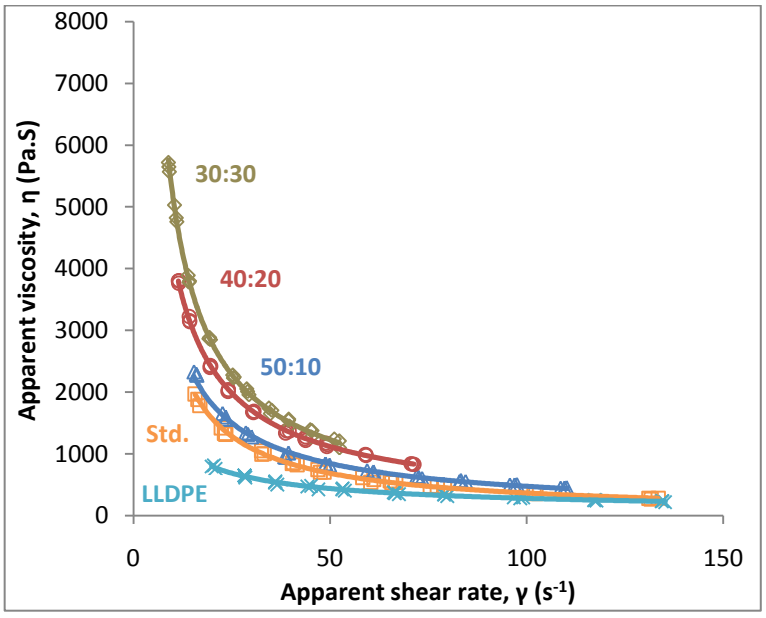

Figure 59: Apparent viscosity vs. shear rate for four different formulations [Std., 50:10, 40:20, 30:30 & LLDPE] at 125°C

In Figure 60, Figure 61 and Figure 62, shear rate vs. shear stress curves are shown for the different formulations tested. The power law model for non-Newtonian flow was fitted to these curves and the constants are shown in Table 14.

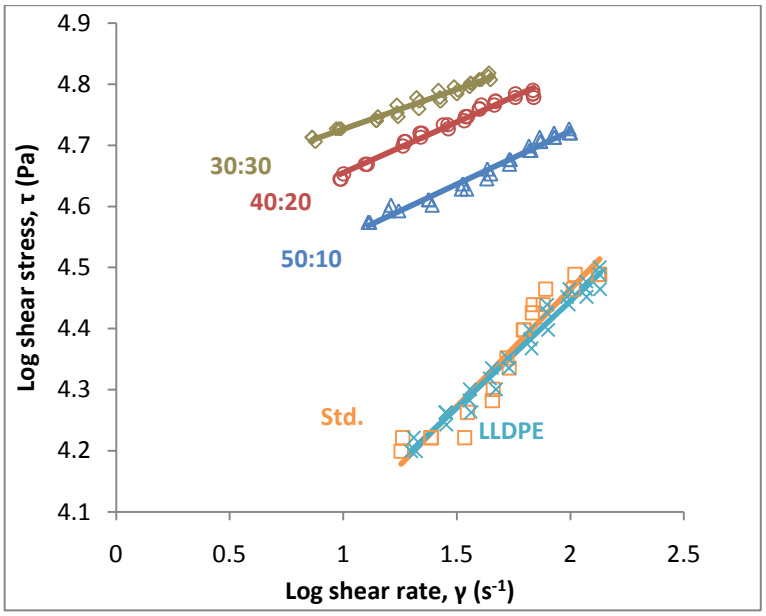

Figure 60: Log shear stress vs. log shear rate for four different formulations [Std., 50:10, 40:20, 30:30 & LLDPE] at 115°C

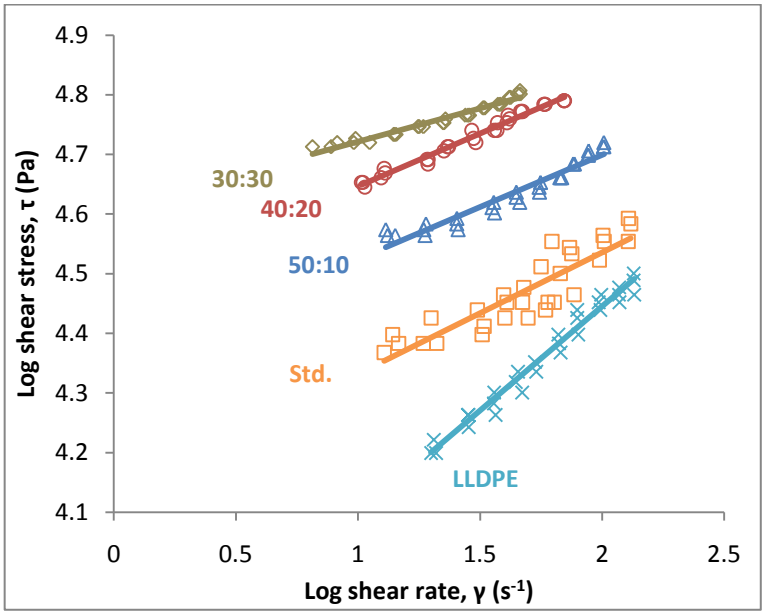

Figure 61: Log shear stress vs. log shear rate for four different formulations [Std., 50:10, 40:20, 30:30 & LLDPE] at 120°C

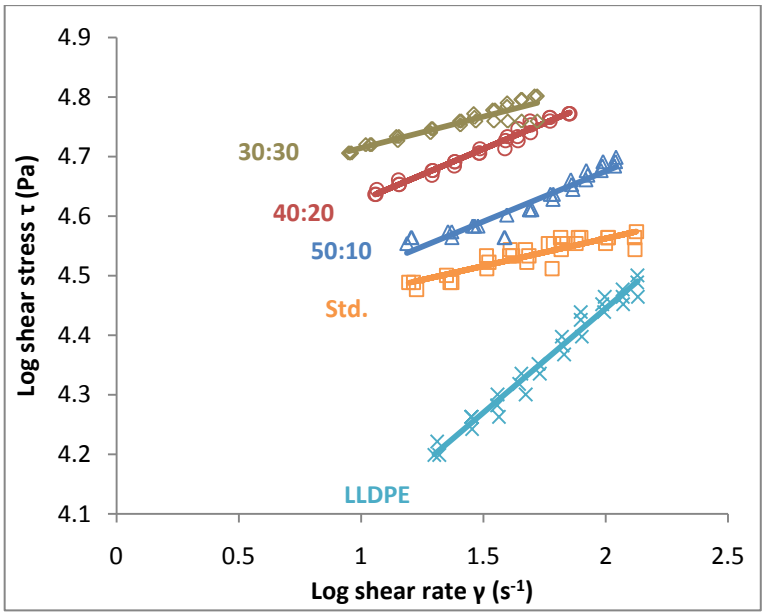

Figure 62: Log shear stress vs. log shear rate for four different formulations [Std., 50:10, 40:20, 30:30 & LLDPE] at 125°C

Table 14: Temperature dependency of NTP (flow behaviour index (slope) and zero shear viscosity values obtained using the power law model)

Temperature (°C)	Flow behaviour index, n (Dimensionless)	K (Pa.s)
Standard		
115	0.38	23824
120	0.20	13455
125	0.09	4968
Formulation 1 [Water (50) : TEG (10)]		
115	0.17	23739
120	0.18	22357
125	0.17	21725
Formulation 2 [Water (40) : TEG (20)]		
115	0.17	30913
120	0.18	29462
125	0.17	28426
Formulation 3 [Water (30) : TEG (30)]		
115	0.13	40648
120	0.11	39483
125	0.11	32293

Moisture and plasticiser content

Standard NTP was used as a reference and contained a total of 70 pph_{BM} plasticiser of which 60 parts were water and 10 parts TEG. In formulations 1, 2 and 3 the total plasticiser content was kept constant at 60 pph_{BM}, but the ratio of water to TEG was varied.

The results shown in the previous figures showed a clear increase in viscosity as the ratio of water to plasticiser was reduced. Of the formulations tested, the standard formulation not only had the highest water to plasticiser ratio, but also contained the highest overall plasticiser content.

Water serves as an effective plasticiser for NTP by forming hydrogen bonding with protein chains and reducing protein-protein interaction. It also increases free volume of the protein molecules, thereby increasing chain mobility which in turn facilitates flowability of the material. Water also facilitates the denaturing action of urea and disulphide bond reduction of sodium sulphite; both of which will improve the flowability of the material. It was therefore not surprising to observe a decrease in viscosity with an increase in water content.

It is important to note that between formulations 1, 2 and 3 the total amount of plasticiser was constant. Despite this, a considerable rise in viscosity was observed when changing the ratio of water to plasticiser. It would appear that water is either a more efficient plasticiser, or that its presence facilitates other mechanisms, as mentioned above. In the absence of sufficient denaturing and crosslink reduction, one would expect a higher viscosity, as evident from the rheology presented here. Although TEG can plasticise NTP, it cannot facilitate

these processes and relies mostly on increasing free volume of the protein network.

The differences between these formulations are more apparent when the shear stress vs. shear rate graphs were considered (Figure 60, 61 and 62). From these graphs it is apparent that the slopes of these curves are very similar, for each temperature tested, with the exception of the standard formulation. This would suggest that the flow behaviour, or degree of non-Newtonian behaviour, is unaffected by the ratio of water to plasticiser. The observed change in viscosity is therefore mostly due to the plasticization effect of water. However, as can be seen from Table 14, the flow behaviour index (n) for the standard formulation was significantly different to the other formulations, suggesting that the higher water content changed the nature of the fluid.

In Equation (27), viscosity was said to follow an exponential relationship with respect to moisture content (C_m).

$$\ln(\eta) = (n-1)\ln(\gamma) + (\ln(k_1) - k_2 T - k_3 C_m) \quad (27)$$

The flow consistency index from the power law model, K (Pa.s) is therefore equal to $\ln(K) = (\ln(k_1) - k_2 T - k_3 C_m)$.

At a given temperature, the slope of a ln (η) vs. ln (γ) graph should therefore be independent of moisture content, but the flow consistency index, K, would be. A plot of ln (K) vs. moisture content, C_m, should therefore be linear, with a slope, k_3. From Figure 63, a linear relationship can be observed between the three formulations tested, but the same relationship is not valid for the standard formulation, for reasons explained earlier.

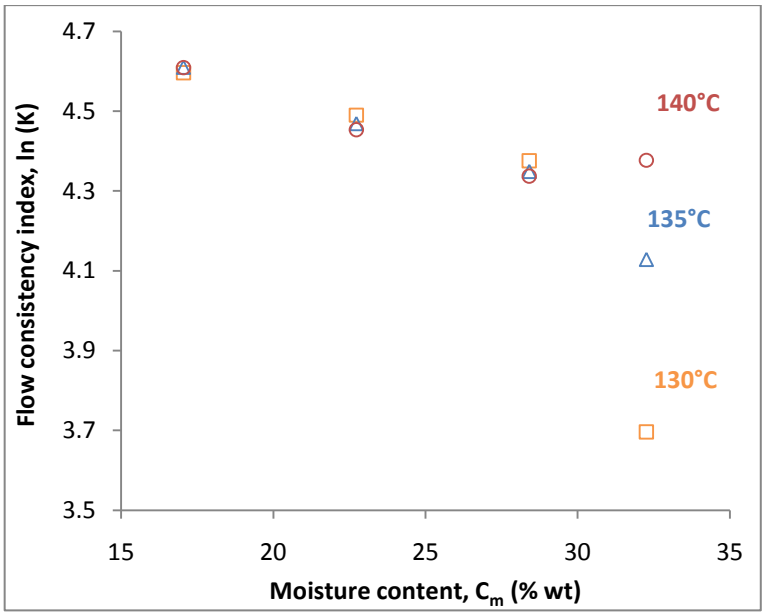

Figure 63: Effect of moisture content

Temperature

The formulations used in this study showed very little temperature dependence, except for the standard formulation. If Equation (33) is used to analyse the temperature dependence of these materials, a plot of ln (K) vs. T, should be linear, with a slope, k_2. It can be seen from Figure 64 that the slopes of the curves for formulations 1 – 3 were almost zero, suggesting very little temperature dependence. However, the standard formulation showed a very strong dependence on temperature, with the zero shear viscosity increasing with temperature.

NTP is known to crosslink at high temperatures due to disulphide (cysteine–cysteine) bonds and will increase the viscosity of the melt. The formation of these bonds is temperature sensitive; increasing with increasing temperature. The ability to form new crosslinks is dependent on the mobility of the chains, which is influenced by moisture content. Standard NTP had the highest moisture content and this could explain the difference in behaviour compared to the other resins. The implication is that the flow behaviour will change with temperature, evident

from changes in the flow behaviour index, n. At low temperature, the standard formulation had the lowest viscosity, probably due to the absence of crosslinking and also a higher overall plasticiser content.

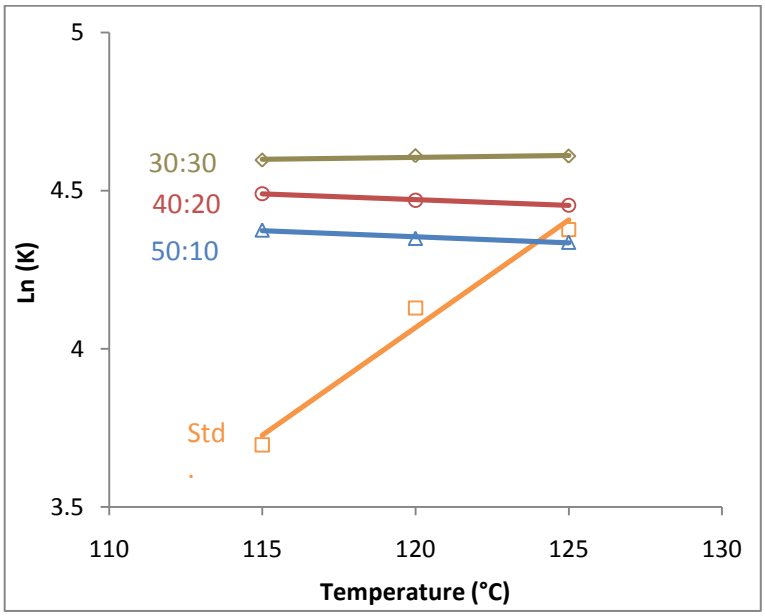

Figure 64: Temperature vs. zero shear stress of shear rate vs. shear stress curves obtained from the Power law model

It has been mentioned earlier that proteins typically have a glass transition close to its degradation temperature. The implication is that chains are not mobile enough at temperatures appropriate for processing. Water and other plasticisers are therefore required to reduce the T_g. In Figure 65, tanδ as a function of temperature is shown for unprocessed bloodmeal, as well as the formulations used in this study. These were determined using DMA, as discussed in Chapter 3. It can be seen that unprocessed bloodmeal had a T_g well above 200 °C and was reduced to about 130 °C when water and TEG was added. The T_gs of the materials were not significantly different. This is expected since the total amount of plasticiser were kept constant (except for the standard formulation, but it was not significantly higher).

According to the WLF equation (Equation 28), the temperature dependence of viscosity is determined by the difference between the operating temperature and its T_g. Only minor changes in T_g were observed for the formulations tested here, explaining the material's insensitivity to changes in temperature. Again the exception is the standard formulation, which contained more water and its behaviour was dominated by other effects.

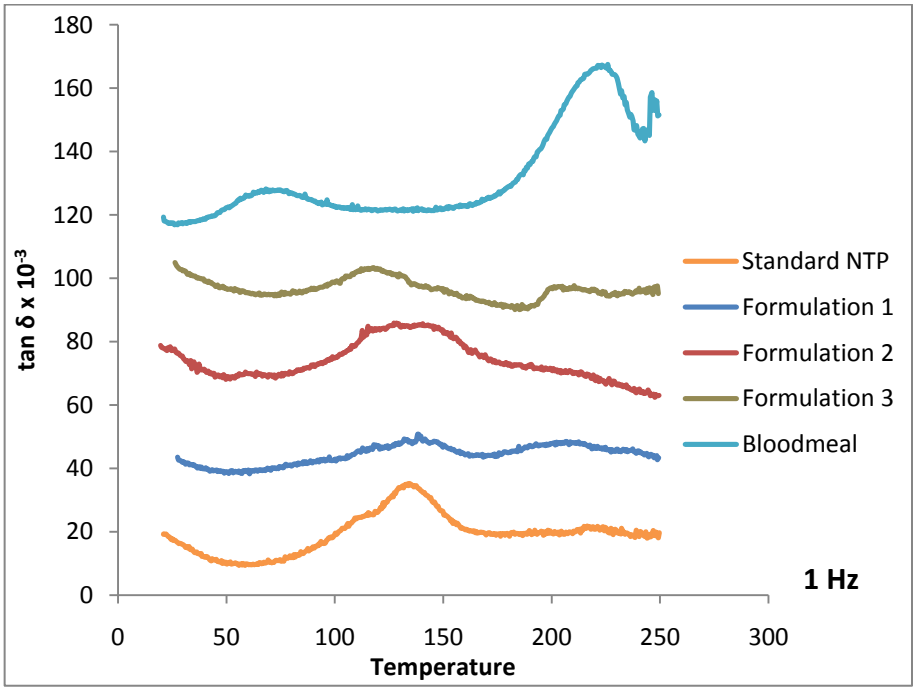

Figure 65: DMA results showing T_g of four different NTP formulations with raw bloodmeal

Pressure drop

The pressure required to force a material through a capillary is proportional to the material's viscosity. In Figure 66, Figure 67 and Figure 68 shear rate is shown as a function of pressure drop at each of the temperatures tested. At 115 °C, it is clear that the required pressure drop for standard NTP and the pressure drop for LLDPE (at 130 °C) were very similar. Considerably high pressure drops were required for all other NTP formulations at 115 °C.

Comparing the behaviour at 115 °C with 120 and 125 °C, the difference between the standard and other formulations is again highlighted. It was observed that the difference between these formulations became less severe with increase in temperature, presumably due to crosslinking becoming more prominent in the standard formulation.

Changing the water to plasticiser ratio leads to increased pressure drop required for the same shear rate. This was mainly due to the effect water which is required for denaturing and efficient chain mobility.

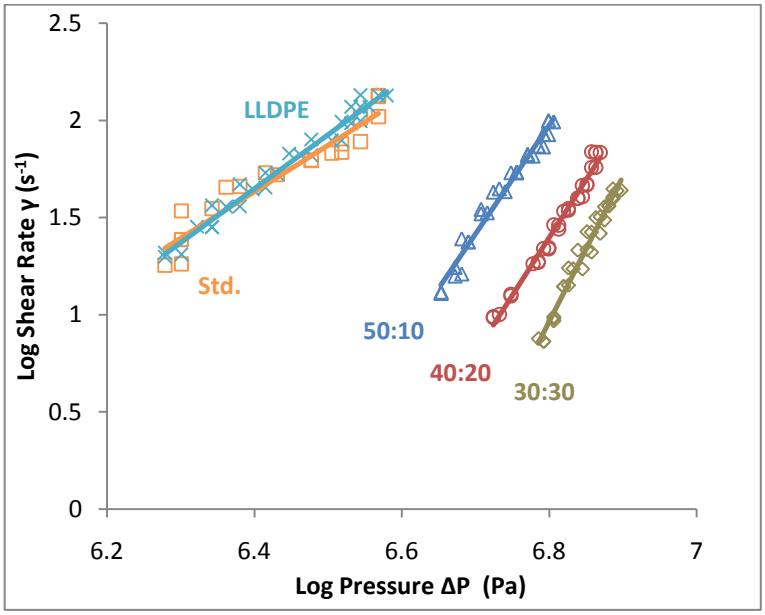

Figure 66: Log shear rate vs. log pressure drop for four different formulations [Std., 50:10, 40:20, 30:30 & LLDPE] at 115°C

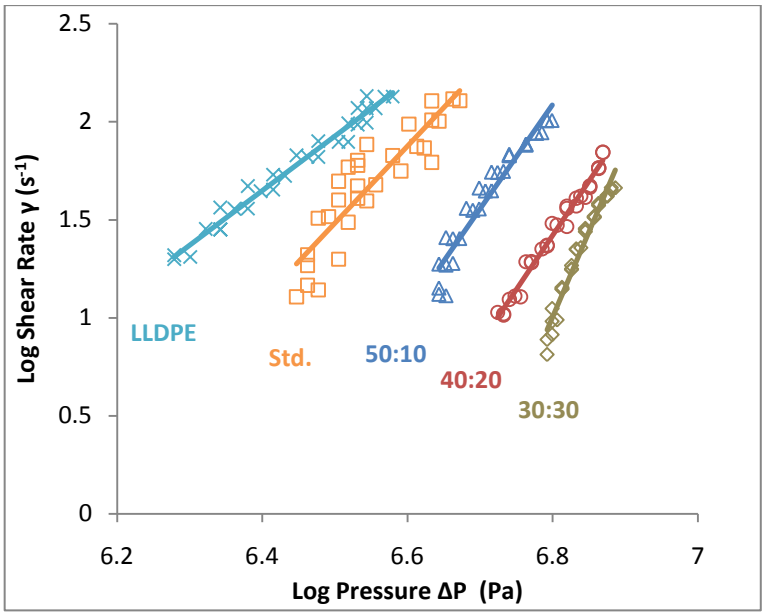

Figure 67: Log shear rate vs. log pressure drop for four different formulations [Std., 50:10, 40:20, 30:30 & LLDPE] at 120°C

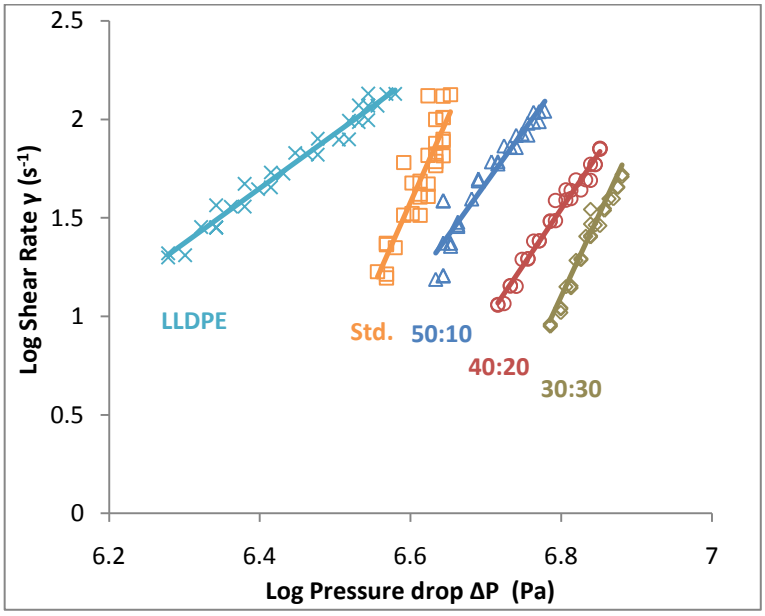

Figure 68: Log shear rate vs. log pressure drop for four different formulations [Std., 50:10, 40:20, 30:30 & LLDPE] at 125°C

True shear rate and true shear stress

Entrance and exit effects were not considered to determine the true viscosity of NTP. Only one capillary was used (L/R = 8.5) and only the effect of temperature and moisture were considered. Hence, Bagley corrections (for shear stress),

Rabinowitsch (for shear rate) and Mooney analysis (wall slip) were not considered. However Rabinowitsch correction could be used to calculate true shear rate, but using this in combination with apparent shear stress would lead to wrong results.

In conclusion to this section:

- NTP behaved like a shear thinning, non-Newtonian fluid.
- The amount of water in NTP had a significant effect on viscosity; a reduction in water content increased viscosity of the material.
- By replacing water with TEG did not fully mitigate the loss of plasticization by water.
- The viscosity of NTP was found to be mostly temperature independent, except for the standard formulation which contained more water.

(Collected data from experiment and sample calculations for LLDPE are given in Appendix 1).

4.2 BATCH MIXER

The processing window for NTP was assessed using a batch mixer equipped with a torque sensor. The same formulations used for capillary rheometry were used here in order to analyse effect of plasticiser, moisture content and temperature.

LLDPE was tested in batch mixer and the results compared to NTP. Figure 69 shows the batch mixer data for LLDPE. When the material was charged in the mixing chamber a sudden rise in torque was observed followed by steady state mixing. Within the maximum time as allowed for NTP (discussed later), the torque did not show any further changes.

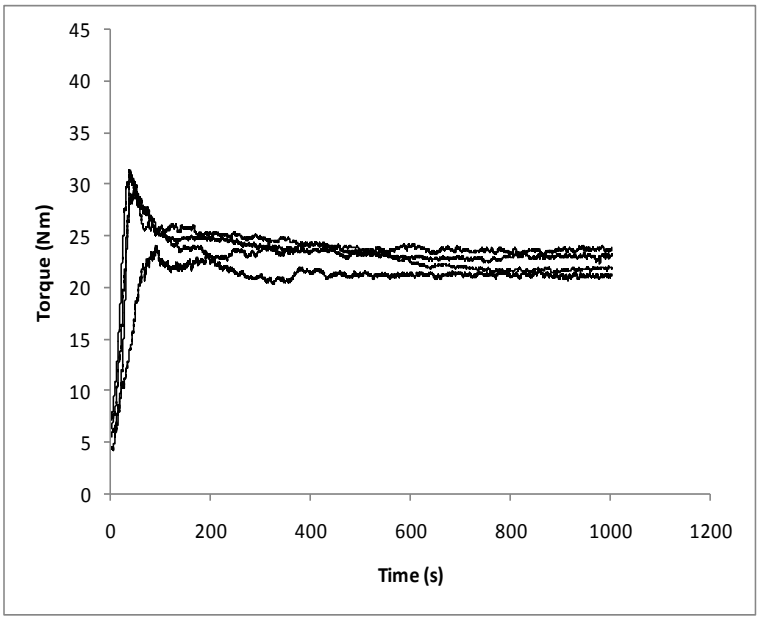

Figure 69: Torque vs. time for LLDPE at 130°C with four RPMs studied (50, 75, 85, 95)

Consolidation of modified bloodmeal powder relies on the application of sufficient shear at high enough temperatures to allow chain movement.

It was found that formulation 3 [water (30):TEG (30)] could not be consolidated in the batch mixer, most likely due to a combination of low water content and insufficient shear. At 115°C, the other formulations only consolidated at 75 RPM and above. This implied that as temperature was reduced more shear was required for consolidation.

Typical torque vs. time graphs for the formulations tested (75 RPM and 115°C) are shown Figure 70. Three regions can be indentified; (1) an induction period, (2) consolidation during with a steady increase in torque was observed (3) torque decay after the material crosslinked and further mixing was impossible. Similar results were obtained in many other protein polymers as discussed in Section 2.6.2.

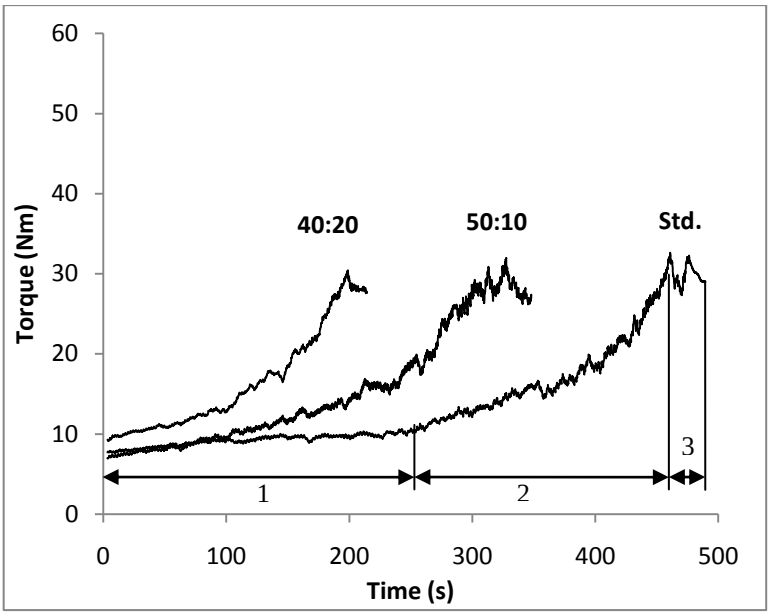

Figure 70: Torque vs. time for three NTP formulations at 75 RPM and 115°C [standard, formulation 1 (50:10), formulation 2 (40:20)]

It was noticed that, the maximum torque was always in the range of 40 to 50 Nm regardless of temperature, RPM and formulation. It was therefore not used in further analysis. It would also indicate that all the materials crosslinked to the same rigid network structure.

4.2.1 Processing window (Δt)

In Figure 71, 72 and Figure 73, the processing windows for three formulations that did consolidate are shown as a function of RPM.

Processing window shortens with increase in RPM. Energy is required for polymer chains to move. The energy can be thermal or mechanical. Higher shear means more efficient mixing and chain rearrangement. This leads to a shorter time between the onset to consolidation and crosslinking because chain molecules are free to move and react.

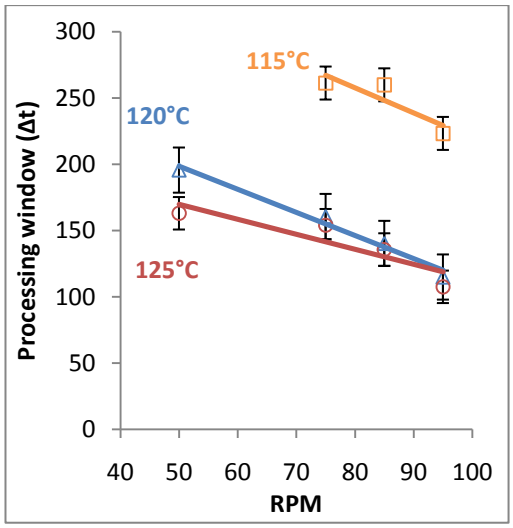

Figure 71: Processing window vs. RPM for standard NTP

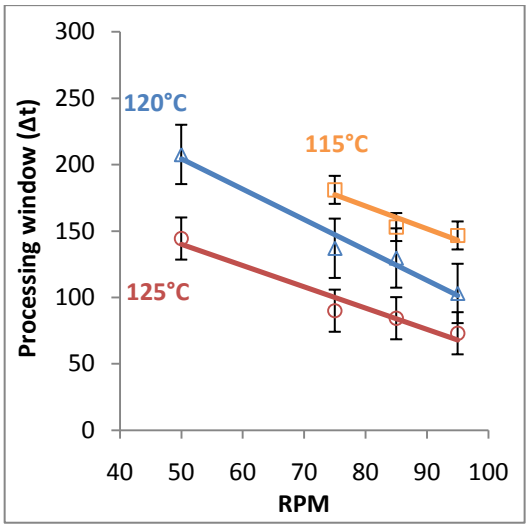

Figure 72: Processing window vs. RPM for NTP formulation 1

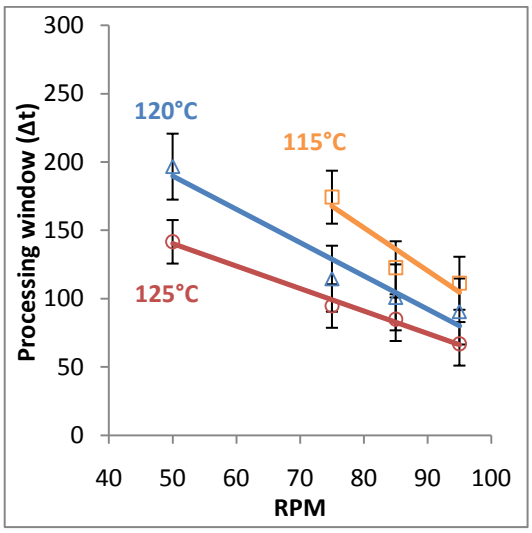

Figure 73: Processing window vs. RPM for NTP formulation 2

For standard NTP at 115°C, the process window is much longer than other formulations as this formulation is highly plasticised with largest water content. Water reduces viscosity leading to a lower shear rate. High shear typically leads to faster crosslinking.

For all the formulations tested, Δt reduces with increasing temperature. High temperature accelerates crosslinking as more energy is available for free movement and diffusion of chain molecules.

They way in which Δt decreases with an increase in RPM is not dependent on temperature, i.e. the slope of the curves shown in the figures are almost same. This means temperature and moisture content are independent It can also be observed that the processing window did not change much between different formulations, except for the standard formulation. The processing window was insensitive to the amount of water, but was slightly longer for the standard formulation that contained an overall larger amount of plasticisers. (Processing window for each formulation at different processing conditions is given in Appendix 4, Table 19).

4.2.2 Onset to consolidation

In Figure 74, Figure 75 and Figure 76 onset to consolidation vs. RPM is shown for the formulations tested. It can be observed that the onset to consolidation decreased with an increase in RPM and temperature. The same mechanisms are important in this case: Sufficient energy is required for chain rearrangement which leads to consolidation. Energy can be supplied either as thermal or mechanical energy.

Very little difference in onset between the various formulations were observed, suggesting that the ratio of water to TEG is not as important during mixing as it was to determining viscosity.

It can be concluded that temperature and shear are the most significant factors influencing the time to consolidation. Alternatively, reducing the total amount of plasticisers (water + TEG) the time to consolidation can also be reduced.

Furthermore, time to consolidation and the processing window cannot be adjusted independently. The time to consolidation was always about 40-50% (Appendix 4, Table 20) of the time to reach maximum torque, when the processing window was reduced, so was the time to consolidation. The manner, in which these changes was constant suggesting same mechanism affect both. (Complete batch mixing data is given in Appendix 2 and maximum time to torque graphs are shown in Appendix 3).

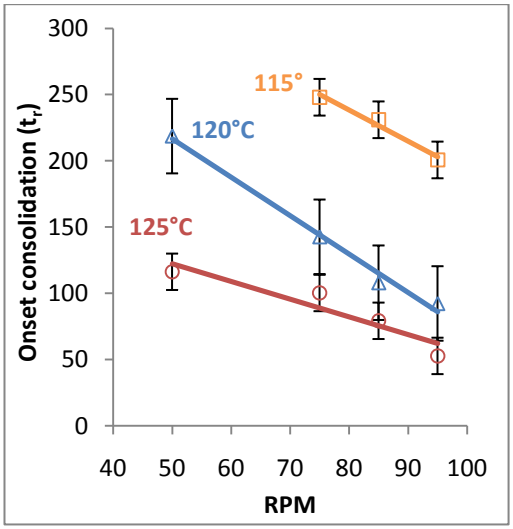

Figure 74: Onset to consolidation vs. RPM for standard NTP

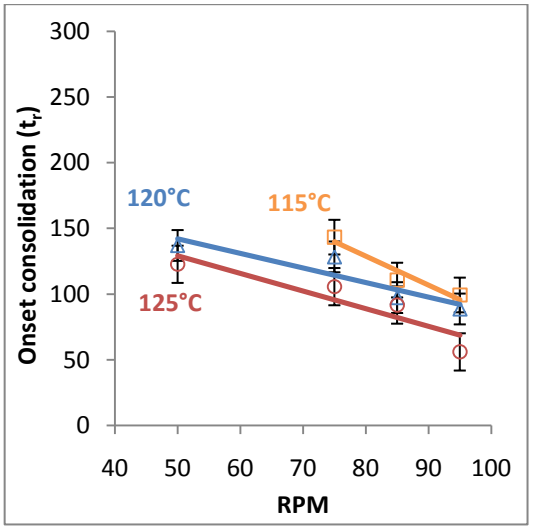

Figure 75: Onset to consolidation vs. RPM for formulation 1

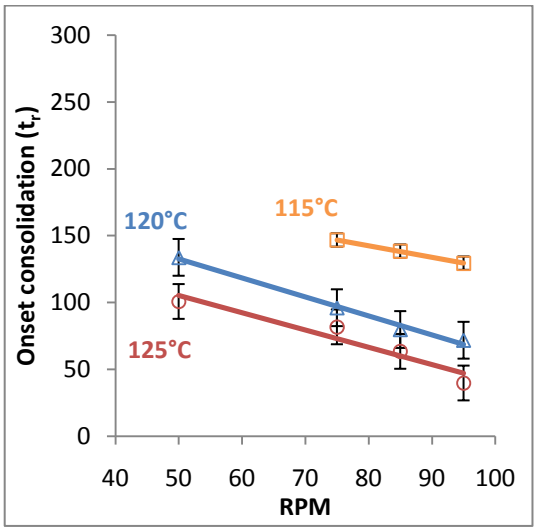

Figure 76: Onset to consolidation vs. RPM for formulation 2

When comparing with LLDPE results, similar behaviour could not be seen with NTP. There was a long steady state region observed in LLDPE, but not with NTP. In protein thermoplastics, crosslinking occurs during mixing thereby leading to a continuously changing viscosity. In capillary rheometry, measurements correspond to a very small period of time, compared to batch mixing since the residence time in the capillary was very short. If a very long capillary were used, the degree of crosslinking will change as the material flow through the capillary. The observed flow behaviour may not be a true fluid property, but rather an effect of chemical reactions.

CHAPTER 5: CONCLUSIONS AND RECOMMONDATIONS

The objective of this research was to assess the processability of Novatein Thermoplastic Protein (NTP) by characterising its rheology using capillary rheometry and batch mixing. From literature, it was shown that most protein-based thermoplastics displayed non-Newtonian, shear thinning behaviour and their viscosity changed with moisture content, temperature and plasticiser content.

In this study, the viscosity of NTP at different water to plasticiser ratios was studied and the following conclusions were made using the results obtained from capillary rheometry:

- Flow behaviour was non–Newtonian and shear thinning.
- The glass transition temperatures of all the formulations (prior to extrusion) were similar, suggesting that the overall plasticiser content was more important than the ratio of water to TEG.
- Viscosity was strongly dependent on moisture content; increasing with decreasing moisture content.
- Viscosity reduced slightly with increasing temperature.
- The degree of non-Newtonian behaviour (n) was not influenced by temperature or moisture content, except for the standard formulation which contained a larger amount of plasticiser.

Torque vs. time data from batch mixing was used to determine time to consolidation and time to crosslinking and the following conclusions were made:

- The processing window decreased with reducing moisture because of increased shear that promotes crosslinking.
- Crosslinking is temperature dependent leading to shorter processing windows with increasing temperature.
- The processing window reduced linearly with RPM because higher shear rates promotes crosslinking.
- Increased mechanical or thermal energy leads to faster consolidation and crosslinking.
- Time to consolidation and the processing window cannot be varied independently and time to consolidation was always about 40 - 50% of the total processing time.

When comparing capillary and batch mixer results, it can be concluded that NTP's viscosity is a function of temperature and moisture content. Processing is dependent on the degree of crosslinking, which changes during processing. The processing window defines the rate of crosslinking, which is faster at lower moisture content and higher temperature and shear.

It is recommended that experiments be performed using capillaries of different length to diameter (L/D) ratios in order to assess entrance and exit effects. Furthermore, longer capillaries my also reveal aspects of protein crosslinking, not observed in this study.

Performing capillary experiments at higher shear rates may also enable a deeper understanding of the rheology of proteins, but much larger pressures are needed and require more specialised equipment.

Blending NTP with other polymers may decrease the viscosity further and may assist in reducing the water dependence of processesability.

CHAPTER 6: REFERENCES

[1] Alfonso Jimemez, Gennady E. Zaikov (2009), *Recent Advances In Research on Bio degradable Polymers and Sustainable Composites,* Nova Science Publishers, 1, 32-42.

[2] Annelise E Barron, Ronald N Zuckmann (1999), *Bioinspired polymeric materials in between proteins and plastics,* Current Opinion in Chemical Biology, 3, 681-687.

[3] Bernard Nathalie Gontard and Stephane Guilbert (1998), *Proteins As agricultural polymers for packaging production,* American Association of Cereal Chemists, Inc., 75 (1), 1-9.

[4] Andreas Redl (1999), *Extrusion of wheat gluten plasticised with glycerol: Influence of Process Conditions on flow behaviour, rheological properties and molecular size distribution,* American Association of Cereal Chemists, Inc., 76 (3), 361-370.

[5] Casparus J.R. Verbeek and Lisa E. van den Berg. (2009), *Recent Developments in Thermo-Mechanical Processing of Proteinous Bioplastics,* Recent Patents on Materials Science, 2, 171-189.

[6] Lisa E. Van den Berg, Casparus J. R. Verbeek (2009), *Development of 2nd generation proteinous Bioplastics,* WaikatoLink Limited, New Zealand.

[7] Verbeek, C.J.R. and L.E. van den Berg (2009), Extrusion Processing and Properties of Protein-Based Thermoplastics, Macromolecular Materials and Engineering, 295(1), 10-21.

[8] Abel Jerez, Pedro Partal, Inmaculada Martínez, Críspulo Gallegos, and Antonio Guerrero. (2007), *Protein-based bioplastics: effect of thermo-mechanical processing,* Rheol Acta, 46, 711–720.

[9] Bousmina, M., Ait-Kadim, A. and Faisant, J.B. (1999), *Determination of shear rate and viscosity from batch mixer data,* Journal of Rheology, 43 (2), 415-433.

[10] Catia Bastioli (2005), *Handbook of Bio Degradable Polymers,* Raora Technology Linited, 1st edition.

[11] Stoyko Fakirov, Debes Bhattacharyya (2007), *Handbook of engineering biopolymers: homopolymers, blends, and composites,* Hanser.

[12] Protein structure. http://barleyworld.org/css430_09/lecture%209-09/figure-09-03.JPG (Retrieved 18. 6.2010).

[13] David Whiteford (2005), *Proteins-Structure and Function,* Whiley, 1st Edition.

[14] David J. Sessa, Gordon, W. Selling, J.L. Willett and Debra E. Palmquist (2006), *Viscosity control of zein processing with sodium dodecyl sulphate,* Industrial Crops and Products, 23, 15–22.

[15] Rishi Shukla and Munir Cheryan (2001), *Zein: The industrial protein from corn,* Industrial Crops and Products 13, 171–192.

[16] Oscar Solar, Sundaram Gunasekaran (2010), *Rheological properties of rennet casein-whey protein gels prepared at different mixing speeds,* Journal of Food Engineering 99, 338–343.

[17] Tom Brenner, Taco Nicolai and Ragnar Johannsson (2009), *Rheology of thermo-reversible fish protein isolate gels,* Food Research International, 42, 915–924.

[18] Justin R. Barone, Walter F. Schmidt and Gregoire N. T. (2006), *Extrusion of feather keratin,* Journal of Applied Polymer Science, 100 (2), 1432-1442.

[19] Ralston, B. E. and Osswald, T. A. (2008), *Viscosity of Soy Protein Plastics Determined by Screw-Driven Capillary Rheometry,* Journal of Polymer Environmental Science, 16,169-176.

[20] Hao Wang, Lin Jiang, Lei Fu (2007), *Properties of Molded Soy Protein Isolate Plastics*, Journal of Applied Polymer Science, 106, 3716–3720.

[21] Rachel Lutz, Abraham Aserin, Yariv Portnoy, Moshe Gottlieb and Nissim Garti (2009), *On the confocal images and the rheology of whey protein isolated and modified pectins associated complex*, Colloids and Surfaces B: Biointerfaces, 69, 43–50.

[22] Jerez, A., Partal, P., Mart´ınez, I., Gallegos, C. and Guerrero, A. (2005), *Rheology and processing of gluten based bio plastics*, Biochemical Engineering Journal, 26, 131–138.

[23] Marion Pommet, Andreas Redl, Marie-Helene Morel and Stephane Guilbert (2003), *Study of wheat gluten plasticization with fatty acids*, Polymer, 44, 115-122.

[24] Hailin Lin, Sundaram Gunasekaran (2010), *Cow blood adhesive: Characterization of physicochemical and adhesion properties*, International Journal of Adhesion & Adhesives, 30, 139–144.

[25] Suraj Sharma, James N. Hodges, Igor Luzinov. (2008), *Biodegradable Plastics from Animal Protein Coproducts: Feathermeal*, Journal of Applied Polymer Science, 110, 459-467.

[26] Gonzalez-Gutierrez, J., Partal, P., Garcia-Morales, M., Gallegos, C. (2009), *Development of highly-transparent protein/starch-based bioplastics*, Biresource Technology, Elsevier Limited.

[27] Olivier Orliac, Francoise Silvestre, Antoine Rouilly, and Luc Rigal (2003), *Rheological Studies, Production, and Characterization of Injection-Molded Plastics from Sunflower Protein Isolate*, Ind. Eng. Chem. Res., 42, 1674-1680.

[28] Abdellatif Mohamed, Girma Biresaw, Jingyuan Xu, Mila P. Hojilla-Evangelista and Patricia Rayas-Duarte (2009), *Oats protein isolate:*

Thermal, rheological, surface and functional properties, Food Research International 42, 107–114.

[29] Brydson, J. A. (1999), *Plastics Materials*, Butterworths 9th Edition.

[30] Morton-Jones, D.H. (1989), *Polymer Processing,* Chapman and Hall.

[31] Peter C. Powell, Jan Ingen Housz, A. (1998), *Engineering with Polymers,* Stanley Thrones Ltd, 2nd Edition.

[32] Osswald, Tim, A., Lih-Sheng Turng, Paul J. Gramamn (2007). *Injection Molding Handbook*. Hanser Verlag. 2nd Edition.

[33] McCrum, N.G., Buckley, C.P. and Bucknall, C.B. (1997), *Priciples of Polymer Engineering, Oxford Science Publications,* 2nd Edition.

[34] Manas Chanda and Sail K. Roy (2007), *Plastics Technology Handbook,* CRC press, 4th Edition.

[35] Sanjay K. Mazumdar (2002), *Composites Manufacturing: Materials, Product, and Process engineering,* CRC Press.

[36] Chhabra, R.P. and Richardson, J.F. (2008), *Non-Newtonian Flow and Applied Rheology,* Elsevier Ltd, 2nd Edition.

[37] Manas Chanda, Salil K. Roy (2009), *Plastic Fundamentals, Properties, and Testing,* CRC press.

[38] Grellmann, Seidler (2007), *Polymer Testing Methods,* Hanser.

[39] Donald G. Baird, Dimitris I. Collias (1998), *Polymer Processing-Principles and Design,* Wiley Inter Science.

[40] Sankar Subramanian, R., Non-Newtonian flow- A review (http://web2.clarkson.edu/projects/subramanian/ch301/notes/nonnewtonian.pdf).

[41] J.M.G. Cowie, Valeria Arrighi (2008), *Polymers: Chemistry and Physics of Modern Materials*, Taylor & Francis Group, 3rd Edition.

[42] Yunus A. Cengel, Robert H. Turner and John M. Cimbala (2008), *Fundamentals of Thermal-Fluid Sciences*, McGraw Hill, 3rd Edition.

[43] Li, T.Q. and Wolcott, M.P. (2005), *Rheology of Wood Plastics Melt. Part1. Capillary Rheometry of HDPE Filled With Maple*, Polymer Engineering And Science, Wiley Inter Science, 549-559.

[44] Leonor Pe´rez-Trejo, Jose´ Pe´rez-Gonza´lez and Lourdes de Vargas. (2001), *About the determination of the steady state flow for polymer melts in capillary rheometers*, Polymer Testing, 20, 523–531.

[45] Goettfert, A. (1986), *Real time viscosity control with capillary rheometer*, German Plastics, 76 (12), 12-14.

[46] van Krevelen, D.W. and Te Nijenhuis, K. (2009), *Properties of Polymers*, Elsevier, 4th Edition.

[47] ASTM Standards: D 5422 – 03, *Standard Test Method for Measurement of Properties of Thermoplastic Materials by Screw-Extrusion Capillary Rheometer*.

[48] Jan J. Tuma, Ronald A. Walsh (1998), *Engineering Mathematics Handbook*, McGraw Hill, 4th Edition.

[49] Bagley, E. B. (1957), *End Corrections in the Capillary Flow of Polyethylene*, Journal of Applied Physics, 285 (5), 624-627.

[50] Kamla, M.R. and Nyun, H. (1973), *The effect of pressure on shear viscosity of polymer melts*, Rheol Acta, 12, 263-268.

[51] Kequan Chen, Jie Shen and Xiaozhen Tang (2005), *Rheological Properties of Poly(trimethylene terephthalate) in Capillary Flow*, Journal of Applied Polymer Science, 97, 705–709.

[52] Faith A. Morrison Michigan Technological University http://www.chem.mtu.edu/~fmorriso/cm4655/lecture_2_cm4655.pdf (Retrieved 24.8.2010).

[53] Wang, Z.Y., Joshi, S.C., Lam, Y.C. and Chen X. (2009), *End pressure correction in capillary rheometry of concentrated suspensions*, Journal of applied polymer science, 114, 1738-1745.

[54] Evan Mitsoulis, Savvas G. Hatzikiriakos, Kostas Christodoulou and Dimitris Vlassopoulos (1998), *Sensitivity analysis of the Bagley correction to shear and extensional rheology*, Rheol acta 37, 438-448.

[55] Jan-Chan Huang and Hsiao-Fu Shen (1989), *Pressure effect in capillary rheometer,* Advances in polymer technology, 9 (3), 211-215.

[56] Bernard Nathalie Gontard and Stephane Guilbert (1998), *Proteins As agricultural polymers for packaging production,* American Association of Cereal Chemists, Inc., 75 (1), 1-9.

[57] Black, W. B. and Graham, M.D. (1996), *Wall-slip and polymer-melt flow instability*, Phys. Rev. Lett., 77, 956-959.

[58] Wall slip, http://www.engr.wisc.edu/groups/fsd/research/slip/ (Retrieved 24.8.2010).

[59] William Brian Black (2000), *wall slip and boundary effects in polymer shear flows,* PhD dissertation in chemical engineering, University of Wisconsin–Madison. http://www.kulikow.com/project/literature/slip2/black_dissert%5b1%5d.pdf (Retrieved 1.7.2010).

[60] L´eger, L., Hervet, H., Massey, G. and Durliat, E. (1997), *Wall slip in polymer melts,* Journal of Physiscs: Condens. Matter, 9, 7719-7740.

[61] Hans Martin Laun (2003), *Pressure dependent viscosity and dissipative heating in capillary rheometry of polymer melt,* Rheol acta, 42, 295-308.

[62] Gómez-Martínez, D., Partal, P., Martínez, I., and Gallegos, C. (2009), *Rheological behaviour and physical properties of controlled-release*

gluten-based bioplastics, Bio Resource Technology, Elsevier Limited, 100, 1828–1832.

[63] Li, T.Q. and Wolcott, M.P (2005), *Rheology of Wood Plastics Melt. Part1. Capillary Rheometry of HDPE Filled With Maple, Polymer Engineering And Science.*

[64] Yi-Dong Li, Jian-Bing Zeng, Wen-Da Li, Ke-Ke Yang, Xiu-Li Wang, and Yu-Zhong Wang (2009)., *Rheology, Crystallization, and Biodegradability of Blends Based on Soy Protein and Chemically Modified Poly(butylene succinate),* Ind. Eng. Chem. Res., 48, 4817–4825.

[65] John Vlachopoulos and David Strutt., *The Role of Rheology in Polymer Extrusion- A review.*

[66] Kevin P. Menard (2008), *Dynamic Mechanical Analysis,* CRC Press, 2nd Edition.

[67] Carlos Bengoechea, Abdessamad Arrachid, Antonio Guerrero, Sandra E. Hill, John R. Mitchell., *Relationship between the glass transition temperature and the melt flow behaviour for gluten, casein and soya,* Journal of Cereal Science 45 (2007) 275–284.

[68] Hydrophilicity http://www.wordconstructions.com/articles/technical/hydrophilic.html (Retrieved 21.7.2010).

[69] Shiao-Wei Kuo (2008), *Hydrogen-bonding in polymer blends,* Journal of Polymer Research, 15, 459–486.

[70] Structure of water, http://witcombe.sbc.edu/water/chemistrystructure.html (Retrieved 16.8.2010).

[71] Structure of TEG, http://www.chemicalland21.com/petrochemical/TEG.htm (Retrieved 16.8.2010).

[72] Hertrampf, J.W and F. Piedad-Pascual, Handbook on ingredients for aquaculture feeds (2000), Dordrecht, The Netherlands: Kluwer academic publishers.

[73] Duarte, R. T, Carvalho Simoes, M.C. and Sgarbieri, V.C. (1999), Bovine blood components: Fractionation, composition and Nutrive value, Journal of agricultural and food chemistry, 47 (1), 231-236.

[74] Overton G. (1978), Method of drying blood, U.S.P office, Editor, USA.

[75] David J. Sessa, Gordon W. Selling, J.L. Willett and Debra E. Palmquist (2006), *Viscosity control of zein processing with sodium dodecyl sulphate*, Industrial Crops and Products 23, 15–22.

[76] Verbeek, C. J. and Beg, D. Blood-Derived bioplastics: Plasticization. Novatein/Waikato Link, Hamilton, New Zealand.

[77] Liang, J. Z. and Ness, J. N. (1997), *Studies on Melt Flow Properties of Low Density and Linear Low Density Polyethylene Blends in Capillary Extrusion*, Polymer Testing 16, 173-184.

CHAPTER 7: APPENDIX

Appendix-1

Method of calculation (Capillary sample calculation for LLDPE)

Step 1: Observed data from experiments;

Diameter of capillary = 4.34 mm

Length of the capillary = 130.2 mm

Time =120 seconds

Mass collected = 17.63g

Pressure (P_1) = 20000000 (Pa)

Atmospheric pressure (P_2) = 101325 (Pa)

Density of LLDPE studied = 0.00092 g/mm^3

Mass flow rate = Mass/Time = 17.63/120 = 0.15

Volumetric flow rate (Q) = Mass flow rate/ Density = 0.15/0.00092 = 159.69 mm^3/sec

Step 2:

$$\text{Shear Rate } (\gamma) = \frac{4Q}{\pi R^3} \ (s^{-1}) = \frac{4*159.69}{\pi\,(4.34/2)^3} = 19.91\ s^{-1}$$

Step 3:

Pressure drop (Δp) = (P_1- P_2) = 1898675 (Pa)

Step 4:

$$\text{Shear stress } (\tau) = \frac{\Delta P\ R}{2L}\ (\text{Pa}) = \frac{1898675*\frac{4.34}{2}}{2*130.2} = 15822.29\ \text{Pa}$$

Step 5:

$$\text{Apparent viscosity } (\eta) = \frac{\text{Shear stress}}{\text{Shear rate}} = \frac{15822.29*\frac{4.34}{2}}{19.91} = 749.75\ \text{Pa. s}$$

Table 15:Data obtained (Capillary rheometry- LLDPE)

Temperature -130°C												
Time (sec)	**Mass(g)**	**Density (g/mm3)**	**Mass flow rate (g/sec)**	**Q (mm3/sec)**	**Shear Rate (1/sec)**	**P2 (Pa)**	**P1 (Pa)**	**(∆P) P2-P1**	**Shear Stress (Pa)**	**Viscosity (Pa.s)**	**RPM**	**Torque (%)**
120.00	17.63	0.00	0.15	159.69	19.91	2000000.00	101325.00	1898675.00	15822.29	794.76	25	43
120.00	24.98	0.00	0.21	226.27	28.21	2300000.00	101325.00	2198675.00	18322.29	649.54	50	44
120.00	31.88	0.00	0.27	288.77	36.00	2400000.00	101325.00	2298675.00	19155.63	532.10	75	45
120.00	39.17	0.00	0.33	354.80	44.23	2600000.00	101325.00	2498675.00	20822.29	470.75	100	43
120.00	46.98	0.00	0.39	425.54	53.05	2800000.00	101325.00	2698675.00	22488.96	423.91	125	43
120.00	58.88	0.00	0.49	533.33	66.49	3000000.00	101325.00	2898675.00	24155.63	363.30	150	44
120.00	69.91	0.00	0.58	633.24	78.94	3300000.00	101325.00	3198675.00	26655.63	337.65	175	46
120.00	85.68	0.00	0.71	776.09	96.75	3500000.00	101325.00	3398675.00	28322.29	292.73	200	45
120.00	103.78	0.00	0.86	940.04	117.19	3600000.00	101325.00	3498675.00	29155.63	248.79	225	46
120.00	118.99	0.00	0.99	1077.81	134.37	3800000.00	101325.00	3698675.00	30822.29	229.39	250	44

Appendix-2

Table 16: Batch mixer data for standard NTP

RPM ↓	Γ_{max} (Nm)					Γ_r (Nm)					t_{max} (s)					t_r (s)				
Rep's →	**1**	**2**	**3**	**Avg.**	**Std. Deviation**	**1**	**2**	**3**	**Avg.**	**Std. Deviation**	**1**	**2**	**3**	**Avg.**	**Std. Deviation**	**1**	**2**	**3**	**Avg.**	**Std. Deviation**
115°C																				
50	Material did not consolidate and crosslink at these conditions																			
75	44	44	51	46.33	4.04	10	8	7	8.33	1.53	510	510	508	509.33	1.15	240	248	256	248.00	8.00
85	42	39	40	40.33	1.53	10	13	11	11.33	1.53	495	488	490	491.00	3.61	238	230	225	231.00	6.56
95	41	42	40	41.00	1.00	14	14	12	13.33	1.15	430	420	422	424.00	5.29	190	212	200	200.67	11.02
120°C																				
50	46	44	45	45.00	1.00	12	13	14	13.00	1.00	410	408	425	414.33	9.29	220	210	226	218.67	8.08
75	50	44	46	46.67	3.06	14	11	10	11.67	2.08	290	315	305	303.33	12.58	140	150	138	142.67	6.43
85	42	46	37	41.67	4.51	14	14	15	14.33	0.58	240	250	255	248.33	7.64	130	90	104	108.00	20.30
95	41	45	51	45.67	5.03	10	11	10	10.33	0.58	218	200	204	207.33	9.45	85	100	92	92.33	7.51
125°C																				
50	46	44	41	43.67	2.52	9	8	7	8.00	1.00	270	286	282	279.33	8.33	165	148	152	116.25	8.89
75	40	39	46	41.67	3.79	10	6	12	9.33	3.06	260	255	248	254.33	6.03	138	128	135	100.25	5.13
85	43	40	40	41.00	1.73	16	9	10	11.67	3.79	208	215	222	215.00	7.00	100	105	112	79.25	6.03
95	40	44	44	42.67	2.31	11	10	11	10.67	0.58	160	156	165	160.33	4.51	75	66	70	52.75	4.51

Table 17: Batch mixer data for NTP formulation 1 [Water (50) : TEG (10)]

RPM ↓	Γ_{max} (Nm)					Γ_r (Nm)					t_{max} (s)					t_r (s)				
Rep's →	1	2	3	Avg.	Std. Deviation	1	2	3	Avg.	Std. Deviation	1	2	3	Avg.	Std. Deviation	1	2	3	Avg.	Std. Deviation
115°C																				
50	Material did not consolidate and crosslink at these conditions																			
75	44	40	37	40.33	3.51	14	13	14	13.67	0.58	350	358	265	324.33	51.54	135	155	140	143.33	10.41
85	42	40	44	42.00	2.00	15	11	11	12.33	2.31	260	276	255	263.67	10.97	100	112	120	110.67	10.07
95	40	45	44	43.00	2.65	13	10	13	12.00	1.73	240	244	254	246.00	7.21	96	94	108	99.33	7.57
120°C																				
50	44	50	41	45.00	4.58	12	11	11	11.33	0.58	340	344	350	344.67	5.03	158	118	135	137.00	20.07
75	40	36	40	38.67	2.31	10	15	14	13.00	2.65	265	260	271	265.33	5.51	120	125	140	128.33	10.41
85	42	45	38	41.67	3.51	13	14	12	13.00	1.00	225	220	236	227.00	8.19	100	112	80	97.33	16.17
95	43	40	40	41.00	1.73	14	11	10	11.67	2.08	185	190	200	191.67	7.64	80	86	100	88.67	10.26
125°C																				
50	46	44	35	41.67	5.86	16	15	13	14.67	1.53	260	285	256	267.00	15.72	110	126	132	122.67	11.37
75	42	42	40	41.33	1.15	12	12	15	13.00	1.73	190	195	202	195.67	6.03	100	115	102	105.67	8.14
85	40	44	41	41.67	2.08	12	11	11	11.33	0.58	180	176	172	176.00	4.00	90	85	100	91.67	7.64
95	39	42	35	38.67	3.51	10	10	11	10.33	0.58	115	140	132	129.00	12.77	50	60	58	56.00	5.29

Table 18: Batch mixer data for NTP formulation 1 [Water (40) : TEG (20)]

RPM ↓	Γ_{max} (Nm)					Γ_r (Nm)					t_{max} (s)					t_r (s)				
Rep's →	**1**	**2**	**3**	**Avg.**	**Std. Deviation**	**1**	**2**	**3**	**Avg.**	**Std. Deviation**	**1**	**2**	**3**	**Avg.**	**Std. Deviation**	**1**	**2**	**3**	**Avg.**	**Std. Deviation**
115°C																				
50	Material did not consolidate and crosslink at these conditions																			
75	41	42	41	41.33	0.58	14	13	15	14.00	1.00	320	325	318	321.00	3.61	140	138	162	146.67	13.32
85	41	42	43	42.00	1.00	14	11	14	13.00	1.73	260	265	258	261.00	3.61	135	142	138	138.33	3.51
95	40	38	40	39.33	1.15	11	16	11	12.67	2.89	240	244	238	240.67	3.06	135	128	125	129.33	5.13
120°C																				
50	44	42	43	43.00	1.00	11	12	13	12.00	1.00	330	333	328	330.33	2.52	125	146	130	133.67	10.97
75	40	40	40	40.00	0.00	10	12	14	12.00	2.00	200	220	212	210.67	10.07	100	86	102	96.00	8.72
85	40	40	44	41.33	2.31	10	14	14	12.67	2.31	180	190	172	180.67	9.02	70	98	71	79.67	15.89
95	39	37	42	39.33	2.52	10	12	13	11.67	1.53	165	160	162	162.33	2.52	95	62	58	71.67	20.31
125°C																				
50	44	43	41	42.67	1.53	10	11	12	11.00	1.00	230	245	252	242.33	11.24	110	100	92	100.67	9.02
75	40	40	44	41.33	2.31	10	11	14	11.67	2.08	175	180	174	176.33	3.21	80	85	80	81.67	2.89
85	41	40	40	40.33	0.58	12	16	12	13.33	2.31	145	152	148	148.33	3.51	60	64	66	63.33	3.06
95	50	38	40	42.67	6.43	10	11	15	12.00	2.65	110	112	98	106.67	7.57	40	38	41	39.67	1.53

Appendix-3

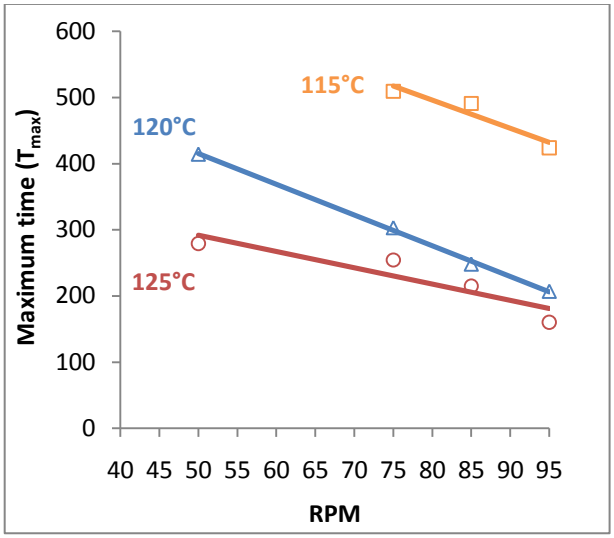

Figure 77: Maximum time to torque for standard NTP

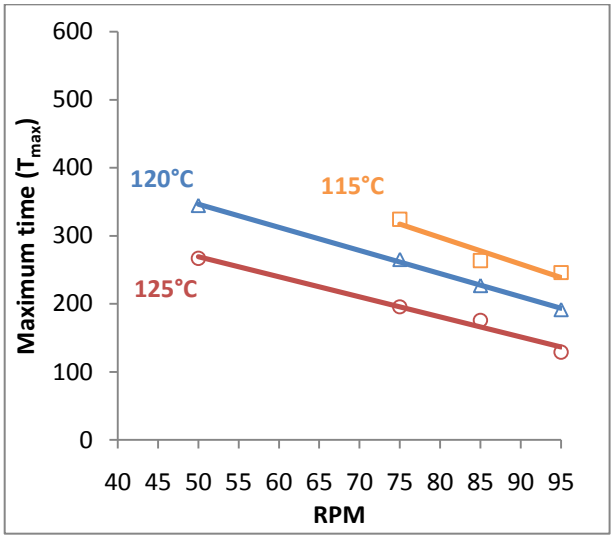

Figure 78: Maximum time to torque for formulation 1

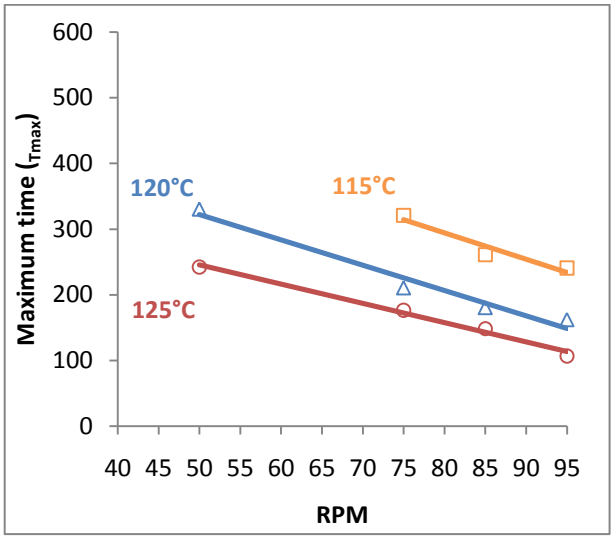

Figure 79: Maximum time to torque for formulation 2

Appendix-4

Table 19: Processing window

Processing window, Δt (s)			
RPM	**Std**	**Formulation 1**	**Formulation 2**
115°C			
50	No action observed		
75	261.33	181.00	174.33
85	260.00	153.00	122.67
95	223.33	146.67	111.33
120°C			
50	195.67	207.67	196.67
75	160.67	137.00	114.67
85	140.33	129.67	101.00
95	115.00	103.00	90.67
125°C			
50	163.08	144.33	141.67
75	154.08	90.00	94.67
85	135.75	84.33	85.00
95	107.58	73.00	67.00

Table 20: Time to consolidation

Time to consolidation, $[(\frac{t_r}{\Delta t + t_r}) \times 100]$ (s)			
RPM	**Std**	**Formulation 1**	**Formulation 2**
115°C			
50	No action observed		
75	48.69	44.19	45.49
85	47.05	41.97	53.00
95	47.33	40.38	53.74
120°C			
50	52.77	39.75	40.46
75	47.03	48.37	45.57
85	43.49	42.88	44.10
95	44.53	46.26	44.15
125°C			
50	41.61	45.94	41.54
75	39.41	54.00	46.31
85	36.90	52.08	42.69
95	32.90	43.41	37.18